DEVELOPMENT OF WHEY PROTEIN ISOLATE BASED NANOCOMPOSITE FOOD PACKAGING FILMS INCORPORATED WITH CHITOSAN AND ZEIN NANOPARTICLES

A Thesis Submitted to
the Graduate School of Engineering and Sciences of
İzmir Institute of Technology
in Partial Fulfillment of the Requirements for the Degree of

MASTER OF SCIENCE

in Materials Science and Engineering

by
Pelin OYMACI

July 2014
İZMİR

We approve the thesis of **Pelin OYMACI**

Examining Committee Members:

Prof. Dr. Sacide ALSOY ALTINKAYA
Department of Chemical Engineering, Izmir Institute of Technology

Prof. Dr. Mustafa M. DEMİR
Department of Materials Science and Engineering, Izmir Institute of Technology

Prof. Dr. Ahmet YEMENİCİOĞLU
Department of Food Engineering, Izmir Institute of Technology

Assoc. Prof. Dr. Fatma Banu ÖZEN
Department of Food Engineering, Izmir Institute of Technology

Assist. Prof. Dr. Ayben TOP
Department of Chemical Engineering, Izmir Institute of Technology

11 July 2014

Prof. Dr. Sacide ALSOY ALTINKAYA
Supervisor, Department of Chemical Engineering
Izmir Institute of Technology

Prof. Dr. Mustafa M. DEMİR
Co-Supervisor, Department of Materials Science and Engineering
Izmir Institute of Technology

Prof. Dr. Mustafa M. DEMİR
Head of the Department of Materials Science and Engineering

Prof. Dr. R. Tuğrul SENGER
Dean of the Graduate School of Engineering and Sciences

ACKNOWLEDGMENTS

I would like to express my deepest thanks to my supervisor Prof. Dr. Sacide Alsoy Altınkaya for her support, guidance and sharing her wisdom throughout my study. I am thankful to Prof. Dr. Mustafa M. Demir, Prof. Dr. Ahmet Yemenicioğlu, Assoc. Prof. Dr. Fatma Banu Özen and Assist. Prof. Dr. Ayben Top for their valuable comments and suggestions. This study was financially supported by Turkish Scientific Technical Research Organization (110M440) which is also gratefully acknowledged.

I also want to express my thanks to Prof. Dr. Ahmet Yemenicioğlu for giving access to tensile tests, Prof. Dr. Mustafa M. Demir for giving access to particle size measurements, Prof. Dr. Metin Tanoğlu for giving access for dynamic mechanical analysis and contact angle mesaurements and Prof. Dr. Funda Tıhmınlıoğlu for giving access to permeability tests. I am also grateful to research assistants Okan Akın, Levent Yurdaer Aydemir, Serkan Kangal and Mehmet Deniz Güneş for their helps in my characterizations. I would also like to thank Biotechnology and Bioengineering Research and Application Center for their support in experiments, Center for Materials Research and Geothermal Energy Research and Application Center for enabling morphological and thermal characterizations.

I am grateful to my workmates Bahar Başak Pekşen Özer, Metin Uz, Melda Büyüköz and Filiz Yaşar Mahlıçlı for their support and friendship. Finally, I would like to express my gratitude to my family for their endless sacrifice, support and motivation.

ABSTRACT

DEVELOPMENT OF WHEY PROTEIN ISOLATE BASED NANOCOMPOSITE FOOD PACKAGING FILMS INCORPORATED WITH CHITOSAN AND ZEIN NANOPARTICLES

The purpose of this study was to investigate the effect of chitosan and zein nanoparticles addition on the barrier and mechanical properties of whey protein isolate (WPI) films as an alternative to conventional synthetic packaging materials. Chitosan nanoparticles (CSNP) were produced via ionic gelation method using sodium tripolyphosphate (TPP) and deacetylated chitosan. Zein nanoparticles (ZNP) were synthesized based on antisolvent procedure in the presence of sodium caseinate (SC) to enable dispersion in water. Both plain and nanoparticle added WPI films were prepared by solution casting method. Water vapor barrier and mechanical properties of films were measured and the improvements in these properties with nanoparticle addition was further investigated through surface wetting, morphological, viscoelastic and thermal properties of the films. Both nanoparticles significantly decreased the water vapor permeability (WVP) and improved the mechanical properties of the WPI film. The highest enhancement in barrier and mechanical properties of the WPI films were recorded with 20% (w/w of WPI) CSNP and 120% (w/w of WPI) ZNP addition which corresponded to the maximum nanoparticle loading levels. At these loadings, the average WVP of pure WPI films loaded with ZNP and CSNP decreased by 84% and 57%, and the average tensile strength increased by 304% and 161%, respectively. On the other hand, the nanoparticles did not change the elongation at break significantly. ZNP was found more effective than CSNP in improving barrier and mechanical properties of the WPI films due to its hydrophobic nature and better dispersion in the protein matrix which allowed much higher loadings compared with the maximum loading levels achieved with CSNP. CSNP addition imparted antibacterial activity to the WPI films.

ÖZET

KİTOSAN VE ZEİN NANOTANECİKLER İÇEREN PEYNİR ALTI SUYU İZOLATI BAZLI NANOKOMPOZİT GIDA AMBALAJI FİLMLERİNİN GELİŞTİRİLMESİ

Bu çalışmanın amacı, kitosan ve zein nanotanecik takviyesinin, geleneksel sentetik ambalaj malzemelerine alternatif biyopolimer bazlı gıda ambalajı olarak peynir altı suyu izolatı (PSİ) filmlerinin bariyer ve mekanik özelliklerine olan etkisini incelemektir. Kitosan nanotanecikler (KNT), sodyum tripolifosfat (STP) ve deasetile edilmiş kitosan kullanılarak iyonik jelleşme metodu ile üretilmiştir. Zein nanotanecikler (ZNT) su ortamında nanotanecik dağılımını sağlayabilmek için sodyum kaseinat (SK) ile birlikte antiçözücü prosedürüne dayalı bir metod ile üretildi. Nanotanecik eklenmiş ve eklenmemiş PSİ filmleri çözelti döküm yöntemiyle hazırlanmıştır. Filmlerin su buharı bariyeri ve mekanik özellikleri ölçülmüş ve daha sonra nanotanecik takviyesiyle bu özelliklerdeki gelişmeler filmlerin yüzey ıslanabilirliği, morfolojik, viskoelastik ve termal özellikleri elde edilerek incelenmiştir. Her iki nanotanecik de PSİ filmlerinin su buharı geçirgenliğini fark edilir ölçüde azaltmış ve mekanik özelliklerini geliştirmiştir. PSİ filmlerinin bariyer ve mekanik özelliklerindeki en iyi iyileşme, en yüksek nanotanecik takviye seviyesi olan %20 (PSİ'ye göre ağırlıkça) KNT ve %120 (PSİ'ye göre ağırlıkça) ZNT katkısıyla kaydedilmiştir. Bu katkı seviyelerinde, ZNT ve KNT eklenmiş saf PSİ filmlerinin ortalama su buharı geçirgenliği sırasıyla %84 ve %57 azalmış; ortalama çekme mukavemetleri de %304 ve %161 artmıştır. Diğer yandan, nanotanecikler kopma noktasındaki uzama değerlerini önemli derecede değiştirmemiştir. ZNT hidrofobik oluşu ve kitosan nanotanecikle sağlanabilmiş en yüksek katkı miktarı ile karşılaştırıldığında daha da yüksek katkı seviyelerinde eklenmesine olanak sağlayan protein matris yapısındaki iyi dağılım göstermesi sayesinde, PSİ filmlerinin mekanik ve bariyer özelliklerini geliştirmede kitosan nanotanecikten daha etkili bulunmuştur. KNT ilavesi PSİ filmlerine antibakteriyel aktivite sağlamıştır.

TABLE OF CONTENTS

LIST OF FIGURES

LIST OF TABLES

CHAPTER 1

INTRODUCTION

There has been an increasing consumer demand for better quality, fresh-like and convenient products, therefore, food packaging becomes important more than ever to provide safe products and minimize food losses. Most of the food packaging materials are based on nondegradable synthetic polymers, thus, represent a serious global environmental problem. In addition, the dependency on fossil resources brings the sustainability problem for raw materials of food packaging production. Biopolymer-based packaging materials represent an alternative to plastic films and they are originated from naturally renewable resources as polysaccharides, proteins, and lipids, from chemical synthesis of bio-derived monomers, such as polylactate; and from polymers naturally produced by microorganisms, such as polyhydroxybutyrate and polyhydroxyvalerate (Wihodo and Moraru 2013). The well-known application of biodegradable polymers in food packaging is as edible films which are used for individual coating of small food products or placed within the food. Biopolymer films can also improve the quality of food products and act as efficient carrier agent for incorporating various additives including antimicrobials, antioxidants, coloring agents, and other nutrients (Wihodo and Moraru 2013).

Economic production of bio-based food packaging materials requires using raw material abundant in nature. Whey protein isolate (WPI) is one of the abundant proteins isolated from milk as a by-product of the manufacture of cheese or casein. Compared to petroleum based synthetic films, WPI has desirable film forming and excellent gas barrier properties (Mchugh et al. 1994; Mchugh and Krochta 1994b; Fairley et al. 1996; Sothornvit and Krochta 2000; Fang et al. 2002; Hong and Krochta 2003; Khwaldia et al. 2004; Perez-Gago et al. 2005; Gounga et al. 2007; Brindle and Krochta 2008; Min et al. 2009). However, its application in food packaging is limited by the low tensile strength, the intrinsic stiffness and poor moisture barrier properties. Various methods have been proposed to overcome inherent shortcomings of WPI based food packaging materials. The most commonly used approaches are blending with other biodegradable polymers (Moditsi et al. 2014; Sharma and Luzinov 2013; Harper et al. 2013; Yoo and Krochta

2011; Wang et al. 2010a; Jiang et al. 2010; Wang et al. 2010b; Brindle and Krochta 2008; Erdohan and Turhan 2005) and lipids (Kokoszka et al. 2010a; Janjarasskul et al. 2014; Min et al. 2009; Perez-Gago and Krochta 2001), coating and lamination (Lee et al. 2008; Hong and Krochta 2006; Hong and Krochta 2004; Hong and Krochta 2003), plasticization (Ramos et al. 2013), pH alteration (Anker et al. 1999), cross-linking by heat, chemicals enzymes or irradiation (Ciesla et al. 2006a; Sabato et al. 2001; Ciesla et al. 2006b). Recent works have also explored the use of nanocomposites to improve the barrier and mechanical properties of WPI films (Sothornvit et al. 2010; Zolfi et al. 2014; Li et al. 2011). The most commonly used nanoparticles as reinforcement agents are based on layered inorganic solids like clays and TiO_2. Sothornvit et al. (2009) prepared WPI based nanocomposite films by blending the polymer with three different types of nanoclays at 5% level: Cloisite Na^+, Cloisite 20A and Cloisite 30B. The nanoclay addition decreased the water vapor permeabilities, however, no significant improvement in mechanical properties was observed. The WPI/Cloisite 30B nanocomposite films showed antimicrobial effect against *L. monocytogenes*. Zhou et al. (2009) reported that small amounts of TiO_2 (<1 %) addition significantly increased the tensile properties of WPI film, on the other hand decreased the moisture barrier properties. Kadam et al. (2013) coated TiO_2 nanoparticles with a layer of silica to prevent aggregation and rapid degradation of the films. Although the addition of inorganic nanoparticles into the WPI matrix brought improvement in film properties, the mechanical and barrier properties are still not satisfactory. Homogeneous distribution of such inorganic nanoparticles in the polymer matrix is not an easy task, therefore, compatibilizing agents are sometimes added or they are chemically modified. In addition, the allowable limits for migration of TiO_2 or nanoclay into food are still unknown.

The objective of the studies in this thesis is to prepare WPI/chitosan and WPI/zein nanocomposite food packaging materials to improve mechanical and water vapor barrier properties of pure WPI films. Specifically, it is aimed to investigate the structural changes in WPI films caused by adding nanoparticles and the effect of these changes on the mechanical and water vapor permeation characteristics of the nanocomposite films. Both chitosan and zein are food-grade polymers which make them appropriate nanoparticles to be used in food packaging with possessing different specific properties. In addition, these nanoparticles are widely used in encapsulating antibacterial and antioxidant materials (Li et al. 2013; Hu et al. 2008) which can add

value to functional properties of WPI films. To the best of our knowledge, this is the first study which proposes the use of chitosan and zein nanoparticles in WPI films.

This thesis consists of 5 chapters. Background information about materials used in this study and literature review were given in detail in Chapter 2. Chapter 3 covers experimental procedure of nanoparticle and film production as well as details of characterization methods. In Chapter 4, results of characterizations were given and discussed in detail by considering the effect of chitosan and zein nanoparticle and finally general conclusions of the study were given at the end of the thesis.

CHAPTER 2

BIOPOLYMER BASED PACKAGING

The main purpose of food packaging is to protect food from its surrounding environment and maintain its quality and increase shelf life. Thus, properties of packaging material play a vital role in the protection of food in many ways. Barrier properties of a packaging material come in the first place since they control the transport of moisture, gases or light into food environment. Moisture and atmospheric gases lead to deterioration of food by oxidative reactions or further microbial contaminations therefore packaging material need to prevent the transfer of moisture and gases. Another important role of packaging is to protect food during handling, transport and storage which require mechanical resistance.

There are many materials used for the production of packaging like papers, clothes, glass and metals. In general, preferred packaging materials are synthetic polymers for many desirable features like transparency, softness, sufficient strength and barrier properties. Polymers commonly used for packaging are listed in Table 2.1 with their oxygen (O_2) and water vapor transmission rates (WVTR). The extensive use of the synthetic polymers in packaging (approximate annual world production is 200 million tonnes, average per capita consumption is 100 kg) due to low cost and satisfying properties have caused serious environmental pollution. In addition, consumption of fossil fuels and increasing petroleum prices, diffusion of residuals in polymers and additives into food together with arising global environmental problems have attracted attention on biodegradable polymers (Mahalik and Nambiar 2010).

Table 2.1. Water vapor and oxygen transmission rates of commonly used polymers in packaging (Source: Woishnis 1995)

Polymer	O_2 Transmission rate (23°C 0% RH) ($cm^3.mm/m^2.day.atm$)	WVTR at 38°C 90% RH ($g.mm/m^2day$)
Poly(ethylene terephthalate)(PET)	1-5	0.5-2
Polypropylene (PP)	50-100	0.2-0.4
Polyethylene (PE)	50-200	0.5-2
Polystyrene (PS)	100-150	1-4
Poly(vinyl chloride) (PVC)	2-8	1-2
Poly(vinyl alcohol) (PVAL)	0.0025	30
Ethylene vinyl alcohol (EVOH)	0.004-0.06 (dry)	1.3-3.4
Poly(vinylidene chloride) (PVDC)	0.015-0.253	0.01-0.08

2.1. Biopolymers as Food Packaging Material

Recent research efforts have focused on the use of biodegradable polymers as alternative packaging materials due to environmental concerns. Biopolymer sources can be classified in three groups: 1) extracted from natural raw materials (2) produced by microorganisms and (3) synthesized from bioderived monomers. Biopolymers of each classification are represented in Figure 2.1. Cellulose, starch, polyhydroxyalkanoates (PHB) and polylactide acid (PLA) are among the acceptable biodegradable polymers representing these groups (Tharanathan 2003).

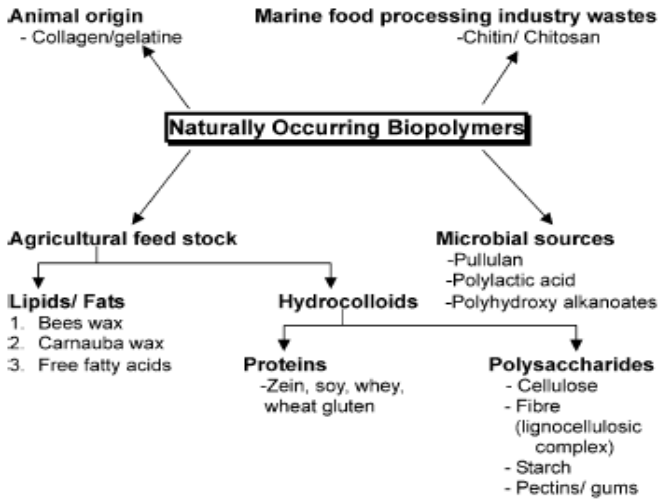

Figure 2.1. Biopolymers of use as packaging films classified according to sources (Source: Tharanathan 2003)

Biopolymers are environmentally-friendly and they can be used for creating innovative packaging materials for enhancing food quality, safety and stability. Table 2.2 summarizes the advantages of natural biopolymer films over traditional synthetic films (Mahalik and Nambiar 2010; Zhang and Mittal 2010).

Table 2.2. Advantages and application areas of natural biopolymer-based packaging materials (Source: Rhim and Ng 2007)

- They are biodegradable
- They can be used as edible coatings
- They can increase the nutritional value of foods enhance its characteristics like appearance, odor and flavor
- They can be used as active packaging with incorporation of antimicrobial agents and antioxidants
- They can control the transfer of moisture, gases, lipids and solutes
- They can be used for microencapsulation and controlled release of antimicrobial agents, antioxidants and active ingredients
- They may be component of a multilayer food packaging materials with non-edible films
- They have low cost
- They are abundant and annually renewable resources
- They are suitable for individual packaging of particulate food such as nuts
- Using them lead to reduced packaging volume, weight and waste
- They can extend shelf life and improve the quality of usually non-packaged items

Biodegradable food packaging materials can be prepared from polysaccharides, lipids and proteins. They have different advantageous properties due to differences in their nature. For instance, proteins and polysaccharides have good barrier properties against oxygen and carbon dioxide in contrast with low barrier properties against moisture due to their highly polar nature. On the other hand, lipids are efficient against moisture but have weak mechanical strength and resistance to gases.

2.2. Polysaccharide Films

Polysaccharides are classified under hydrocolloids and they are known with their structural complexity. Cellulose, starch and chitosan are among the polysaccharides that are investigated as packaging films. Cellulose is the most abundant polymer in nature and it is a cheap raw material. It is highly crystalline and insoluble. Cellulose is derivatized with different modification techniques. Therefore it is a high cost material and difficult to process (Petersen et al. 1999). Carboxymethyl cellulose

(CMC) is derived cellulose and studied as packaging material. It has excellent film forming properties due to the water solubility and compatibility with other biopolymers. Barrier and mechanical properties are better with higher molecular weight of CMC (Tharanathan 2003).

Starch is another biopolymer that is widely investigated as biopolymer which is abundant raw material and relatively low cost material. These polysaccharides are obtained from corn and they exhibit thermoplastic properties. Production methods of starch include extrusion, blow molding and injection molding. Hydrophilic nature of starch makes it sensitive to moisture with moderate gas barrier properties. Starch derived products like dextrin or glucose are used to ferment polylactic acid polymer which is now a popular packaging material. Although it has advantageous such as good performance and easy processing, they have higher cost as compared to synthetic polymers (Petersen et al. 1999).

Chitosan exhibits good free standing films with different modifications such as cross-linking and formation of composite with other polymers. Cross-linked chitosan yields better strength and resistance during handling. Antifungal and antibacterial properties of chitosan also add advantageous functionality to packaging film (Tharanathan 2003).

2.3. Lipid Films

Bees wax, candelilla wax or paraffin are lipids used in formation of films and coatings. For instance, wax coatings are used on fruits and vegetables to prevent the moisture loss and maintain the quality of food. Lipids and fatty acids are also studied with other biopolymers to decrease the sensitivity of biopolymer to moisture due to their hydrophobic nature (Tharanathan 2003).

2.4. Protein Films

Proteins are based on hundreds of amino acids. Depending on combinations of amino acids, secondary, tertiary and quaternary structures occur due to different interactions. The responses of proteins to physical and chemical treatments like heat,

mechanical, pressure, irradiation, lipid interfaces and metal ions differ from each other due to differences in their structures.

Soy protein, wheat gluten, corn zein and whey protein are the most common proteins investigated to develop biodegradable films. Protein films possess intermolecular disulfide bonds, electrostatic bonds, hydrogen bonds and hydrophobic bonds between protein chains. These interactions cause the brittleness of films, thus, requires the use of plasticizer to reduce brittleness and increase film quality. Glycerol, sorbitol, polyethylene glycol, lipids and fatty acids are the generally used plasticizer in the production of protein films. In addition to these, water is another effective plasticizer due to hydrophilic nature of protein films. Plasticizer is a small molecule with low volatility that loosens protein chains by entering between the chains and reducing the attractive interaction which lead to increased mobility of the chains, consequently, decreased glass transition temperatures and increased free volume in the structure. The effect of plasticizer on final properties of the films greatly depends on type, size, shape and compatibility with protein. For instance, hydrophilic plasticizers adsorb more water and cause greater declines in tensile and barrier properties of proteins (Zhang and Mittal 2010). Protein films are formed by cross-linking of polypeptide chains through partial denaturation by the addition of a solvent, an electrolyte, and alteration of pH or application of heat.

2.5. Film Preparation Methods

Biodegradables are processed in two ways to form films: dry and wet process. In dry process, biopolymers are heated and plasticized then extruded or compression molded like thermoplastic polymers. In wet process, film forming solutions are dried following solution casting. Processes can differ depending on the type of material. For instance, lipid and wax films are formed through melting and solidification. On the other hand, coacervation is another process that is used to form biopolymer films. Heat, addition of salt and pH alteration causes to change in the conditions and biopolymers aggregate in a film phase.

Solvent casting is the most widely used technique to produce edible films. Initially, biopolymers are dissolved in a solvent. Then, solution is cast on a substrate

and solvent evaporates in set conditions. It is a commonly used preparation method of whey protein isolate films.

Extrusion is another method in formation of biopolymer films. Biopolymer is extruded at high temperatures and shear applied softens and melts the polymer. As a result, cohesive film matrix is obtained. Extrusion has some advantages over solvent casting method. Extrusion is faster and requires less energy than solvent casting. Evaporation step in solvent casting method is energy and time consuming. In addition, continuous production cost is high due to drying ovens especially for aqueous solutions due to slower evaporation rates than organic solvents (Onwulata and Huth 2008).

2.6. Whey Protein Isolate

Whey is a liquid byproduct of cheese production which is a source of valuable nutritional proteins. It is generated excessively and treated as waste material. For every kilogram of cheese, 9 liters of whey is produced and thus, in a large cheese factory, daily production of whey can reach over 1 million liters (Jelen 2003). Whey is treated at several processes and dried to be obtained in powder form.

Whey protein isolate is the concentrated whey powder containing high percentages of protein (>90%) and water soluble over wide range of pH (Tunick 2008). As can be seen in Table 2.3, WPI has two major components with different molecular weights and conformations resulting in different monomer radii that greatly influence WPI properties: β-lactoglobulin (β-LG) and α-lactalbumin (α-LA). β-LG is globular protein and has molecular weight of 18000 kDa. At pH between 5.2 and 8.0, β-LG exists in non-covalent linked spherical dimer structure. α-LA has lower molecular weight and forms compact, spherical tertiary structure (Onwulata and Huth 2008).

Table 2.3. Whey protein isolate components
(Source: Onwulata and Huth 2008)

Protein type	Amount (%)	Molecular weight (kg/mol)	Isoelectric pH
β-lactoglobulin	48-58	18	5.4
α-lactalbumin	13-19	14	4.4
Glycomacropeptide	12-20	8.6	<3.8
Bovine serum albumin	6	66	5.1
Immunoglobulin	8-12	150	5-8
Lactoferrin	2	77	7.9
Lactoperoxidase	0.5	78	9.6

WPI film can form from native proteins with electrostatic interactions, hydrogen bonding and van der Waals forces between protein chains. Film would be cohesive as water evaporates however it possess weak properties. Therefore, resulting WPI solution needs to be modified and strengthened by cross-linking which is generally achieved by application of heat. As a result of applied heat treatment, proteins in structure of WPI denature and this causes loss of solubility in water. Hidden reactive sites like disulfide linkages and thiol groups in molecular structure of β-LG and α-LA become free by unfolding of the protein and chemical bonding (covalent) at disulfide sites and physical bonding (hydrogen bonding, hydrophobic and electrostatic interactions) occur upon gelation as can be seen in Figure 2.2 (Mehra and O'Kennedy 2008). Denaturation of proteins begins at 40°C and β-LG does not denature until 78°C. Then, 95% of protein denature irreversibly at 85°C and gelation occurs above this temperature (Paulsson and Dejmek 1990; Hong and Creamer 2002;Chaplin and Lyster 1986;Kilara and Vaghela 2004).

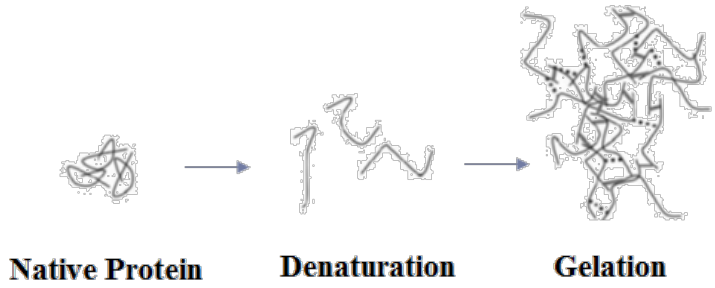

Figure 2.2. Representation of WPI film formation through denaturation
(Source: Onwulata and Huth 2008)

An important factor in denaturation of WPI films is the critical gel concentration (c_g). The c_g is the minimum concentration to form a gel under external factors like heat-induced denaturation for WPI. At the point of gel formation, protein network becomes connected. Due to gelation of WPI at high temperatures and good film forming abilities, WPI has received attention as an alternative food packaging material.

The major production method of WPI film is solvent casting. Dilute biopolymer solution is cast on a surface as a thin layer and then solvent evaporates to form film. Drying method affects the physical properties of the final film. Evaporation of water occurs in two steps during drying. At constant rate period, mass transfer of water occurs between surface of the film and air. When the surface and air conditions are in equilibrium, falling rate period begins. In this period, mass transfer of water from surface of the film to air depends on diffusion of water from the inside of the film to surface. Thus, drying rate is dependent on exposed surface area, drying temperature, relative humidity, drying air velocity and drying period. Other production techniques are microwave drying, infrared drying and extrusion which results in different properties of the final film (Onwulata and Huth 2008).

There are many studies in literature that investigates WPI films. Early studies generally focused on the film forming abilities of WPI depending on the polymer and plasticizer concentration, pH, denaturation temperature and duration and effects of these parameters on permeability and mechanical properties of films. Common parameter that affects both mechanical and barrier properties of WPI film is plasticizer which is usually used to reduce the brittleness of WPI films. Glycerol is one of the commonly used water soluble plasticizer in WPI based films. It has good water solubility, polarity, non-volatility, high boiling point and polymer miscibility. Due to the compatible hydrophilic nature, it increases the flexibility and decreases mechanical strength and barrier properties of the film by favoring the water adsorption through films. There are studies investigating the effects of different plasticizers depending on their molecular weight, amount and polarity. For instance, small molecular weight and polarity provides the ease to plasticizer to move in hydrogen bonding sites, disrupt interactions and enter between chains. Sorbitol is another plasticizer used in whey protein isolate films. Mchugh and Krochta (1994a) studied the different effects of sorbitol and glycerol in WPI properties. Results showed that sorbitol added WPI films exhibited lower permeability results due to less polarity than glycerol but decreased elongation and formed weaker films.

2.6.1. Barrier Properties of WPI Films

Barrier properties are the most important characteristics of food packaging material due to dependence of food quality to amount of water vapor and oxygen in food environment. Moisture and oxygen composition in the food environment should be kept constant therefore packaging material must have certain barrier properties.

Permeation of a gas or vapor through a polymer film takes place in three steps: a) absorption into the polymer b) diffusion through the film c) desorption from the other side of the film. The main driving force for permeation is the concentration difference between two phases. Diffusion through the polymer film is described by Fick's Law in Equation 2.1.

$$J = -D\frac{\delta c}{\delta x} \tag{2.1}$$

where D is the diffusion coefficient and flux of the permeate is represented by J and is proportional to concentration gradient ($\delta c/\delta x$).

When diffusion takes place under steady state conditions and diffusion coefficient does not vary with concentration, then Equation 2.1 can be written as:

$$J = \frac{D\,(c_1 - c_2)}{d} \tag{2.2}$$

where c_1 and c_2 are concentration of penetrant on both side of the film and d is the thickness of the film. The concentrations of penetrant on the film surfaces are related to the ambient penetrant pressure in contact with polymer surface through solubility of penetrant (S) in the film.

$$c = S\,p \tag{2.3}$$

The flux of the permeant can then be obtained by combining Equation 2.2 and 2.3

$$J = \frac{DS(p_1 - p_2)}{d} \tag{2.4}$$

p_1 and p_2 in this equation represent ambient pressures on each side of film with thickness d. DS is permeability coefficient P. If P is substituted in Equation 2.4, flux equation can be obtained in terms of permeability.

$$J = \frac{P\,(p_1 - p_2)}{d} \tag{2.5}$$

P is a material property which is independent from sample geometry, pressure and time. P can be obtained by transmission rate r_t which is measure of volume of gas passing through a membrane with known area per unit time with membrane thickness d and pressure p (Mittal 2009).

$$P = \frac{r_t . d}{p} = \frac{(\text{quantity of permeant}).(\text{film thickness})}{(\text{area}).(\text{time}).(\text{pressure})} \tag{2.6}$$

Moisture and oxygen permeability (O_2P) are most important factors among other gases and vapors for packaging material. Unlike water vapor permeability, WPI films have been determined to be excellent barriers to oxygen permeability. There are many studies in literature investigating the parameters that influences the barrier properties of WPI films.

2.6.2. Mechanical Properties of WPI Films

Packaging material needs to have durable structure to withstand different conditions and to protect its integrity. Tensile strength, elastic modulus and percent elongation are indicators of mechanical properties of a film. As compared to synthetic polymers, WPI films have lower tensile strength. Therefore, these properties need to be improved.

2.7. Strategies to Improve Barrier and Mechanical Properties of WPI Films

WPI has desirable film forming and excellent gas barrier properties; however, its application in food packaging is limited by the low tensile strength, the intrinsic

stiffness and poor moisture barrier properties. Various methods have been proposed to overcome inherent shortcomings of WPI based food packaging materials. The most commonly used approaches are blending with other biodegradable polymers and lipids, coating, lamination, plasticization, pH alteration, cross-linking by heat, chemicals enzymes or irradiation and nanoparticle addition into the film structure. In the following section, the effects of these strategies on the properties of WPI films are reviewed.

2.7.1. Blending With Other Biopolymers

WPI films were blended with many other biopolymers to improve their mechanical and barrier properties. The main difficulty of blending is to obtain homogenous film structures. Sharma and Luzinov (2013) blended whey protein with: natural latex and egg white albumin which are potentially compatible with whey protein since they have amino acids with reactive groups. It was observed that total of about 10% of the latex and albumin addition to the whey improved its toughness characteristics without compromising the strength and stiffness. Yoo and Krochta (2011) investigated the effects of different polysaccharide methylcellulose (MC), hydroxypropylmethylcellulose (HPMC), sodium alginate (SA) and starch with WPI combinations on tensile properties, water vapor permeability (WVP) and oxygen permeability (O_2P) in comparison with pure WPI and pure polysaccharide (PS) properties. No significant difference was observed in WVP of blended, pure WPI and pure PS films. MC and HPMC blends increased O_2P but SA-WPI blend decreased O_2P of pure WPI films. Blending WPI with MC, HPMC and SA increased tensile strength of pure WPI films. Starch-WPI films were weakest among other films. In overall, blended films with WPI and HPMC or MC benefited from superior tensile properties of HPMC or MC and oxygen barrier property of WPI. Prommakool et al. (2011) combined whey protein isolate (WPI) with a hot-buffer-soluble-solid fraction (HBSS) and an alkaline-soluble-solid fraction (ASS) of okra polysaccharides (OKP) to form blend edible films. Compared to WPI film, WPI-HBSS blend films had improved flexibility, stretchability and oxygen barrier. Wang et al. (2010a) reinforced the mechanical strength of the whey protein film with 0.1% sericin addition as a result of the hydrogen bonding between the sericin and whey protein molecules and decreased the WVP of the WPI film with the sericin content. Erdohan and Turhan (2005) blended the WPI film with different

amounts of methylcellulose (MC). Results showed that barrier and tensile properties significantly increased as MC amount increased. Jiang et al. (2010) blended WPI with gelatin at a mass ratio close to 50:50. A discontinuous film structure was observed due to aggregation which led to a decline of the puncture strength of the film and an increase in the WVP of the composite films. Brindle and Krochta (2008) blended the HPMC and WPI at different ratios using glycerol as plasticizer. It is reported that mechanical properties were improved with blending HPMC and WPI compared to pure WPI and HPMC films. Blending of WPI with HPMC did not change O_2P of the film.

2.7.2. Lipid Addition

Blending of biopolymers with different kind of lipids is extensively studied in literature in order to improve film properties. Janjarasskul et al. (2014) added candelilla wax (CAN) into WPI at different ratios to determine its effect on the barrier and tensile properties. Tensile properties were influenced more significantly than the barrier properties with addition of the CAN. Kokoszka et al. (2010a) added different levels of rapeseed oil and observed improvement in moisture barrier properties especially at high humidities. Similarly, Min et al. (2009) observed that when beeswax (BW) was incorporated into WPI films, tensile strength, elastic modulus and WVP of the films decreased. Perez-Gago and Krochta (2001) blended WPI film with 20% and 60% beeswax (BW) and investigated parameters like BW content, particle size and drying temperatures. They reported that effect of particle size is dependent on lipid content and film orientation due to phase separation. As lipid content increased, barrier and tensile properties are improved with decreased particle size due to increase in protein immobilization with increased lipid surface area. However, lipid particle size showed no significant effect at films with phase separation due to overwhelming by dominant effect of increased lipid content.

2.7.3. Crosslinking of WPI Films

Crosslinking is another strategy to improve properties of WPI films. Heat denaturation is a generally used way of cross-linking for WPI but there are other

methods for inducing protein cross-linking. Irradiation was used to cross-link other protein types as stated before by changing molecular weight. However, tyrosine which is the initiator of hypothesized mechanism in irradiation (radical polymerization) is low in whey proteins so that irradiation does not change WPI significantly by itself. Hence, WPI can be cross-linked by irradiation with other proteins like casein. Ciesla et al. (2006a) cross-linked WPI with calcium caseinate (CC) and γ-irradiation and reported that mechanical properties increased while WVP decreased significantly. Ciesla et al. (2006b) further studied the effect of blending γ-irradiated CC-WPI solution with starch and sodium alginate. Better mechanical and barrier properties were achieved when polysaccharides were mixed with formerly irradiated CC-WPI solution.

Other ways of cross-linking whey protein is to use toxic chemicals and enzymes like formaldehyde, glutaraldehyde, tannic and lactic acid. However, usage of these agents is inappropriate. Food grade enzyme that is used to cross-link is transglutaminase (Onwulata and Huth 2008). Cross-linked films are less soluble, thus, degree of cross-linking affect the permeability properties. Sabato et al. (2001) cross-linked the blend of soy protein isolate (SPI) and WPI by means of γ-irradiation combined with thermal treatments. The effect of the incorporation of carboxymethylcellulose (CMC) and poly(vinyl alcohol) was also examined. The mechanical properties of all films were improved by γ-irradiation combined with thermal treatment.

2.7.4. Nanoparticle Addition

Nanotechnology is introduced to food industry in many ways, and the most common application is the preparation of nanocomposite food packaging materials for improving mechanical and barrier properties. Clay and TiO_2 are common inorganic nanoparticles studied so far to produce WPI based nanocomposite films. Zolfi et al. (2014) developed kefiran-whey protein isolate -titanium dioxide (TiO_2) blend films by changing amount of TiO_2 nanoparticles incorporated. Addition of TiO_2 nanoparticles improved moisture barrier properties, but, significantly decreased tensile strength and Young's modulus of the kefiran-WPI films. The main disadvantage of inorganic nanoparticles is dispersion difficulty due to agglomeration at high nanoparticle concentrations which prevents the improvements in film properties. Results also showed that it is not easy to achieve simultaneous improvements in mechanical and barrier

properties. Zhou et al. (2009) studied the effect of TiO_2 nanoparticles in the properties of WPI film. Small amount of TiO_2 nanoparticle (<1 wt %) significantly increased tensile strength but decreased the moisture barrier properties. In contrast, higher TiO_2 concentrations increased the moisture barrier properties and decreased tensile strength. Microstructural characterization revealed the agglomerations occurred in WPI matrix. Li et al. (2011) also incorporated TiO_2 nanoparticles in WPI matrix and reported that addition of 0.25% TiO_2 (w/w of WPI), have increased tensile strength significantly. Although WVP significantly decreased at 1% TiO_2 (w/w of WPI) due to blocking of the path of water vapor by large water insoluble agglomerates in network, large agglomerations decreased the tensile strength. Important advantage of TiO_2 is its photocatalytic activity that gives antibacterial property to film and provide protection against foodborne microorganisms in presence of ultraviolet radiation. Kadam et al. (2013) coated TiO_2 nanoparticles with silica to prevent agglomeration and increased tensile strength. Sothornvit et al. (2009) studied the effect of different nano clay types of Cloisite Na+, Cloisite 20A and Cloisite 30B. No significant difference was observed in tensile properties while moisture barrier properties increased except for addition of Cloisite 20A. In addition, Cloisite 30B in WPI films exhibited antibacterial effect against *Listeria monocytogenes*. Sothornvit et al. (2010) further studied the effects Cloisite 30B amount and reported that WVP decreased as amount of clay increased. However, tensile properties were decreased due to lack of intercalation or exfoliation and brittle nature of clays.

2.8. Chitosan and Zein Nanoparticles

Chitosan (CS) was used in several studies in nanoparticle form for the purpose of improvement in biopolymer properties. Incorporation of chitosan nanoparticles (CSNP) in hydroxypropyl methylcellulose (HPMC) film has been investigated by de Moura et al. (2009). Results showed that the mechanical and barrier properties of the HPMC film were improved through nanoparticle addition by occupying the empty spaces in the pores of HPMC matrix. This study proved that CSNP can be used as an alternative to inorganic nanoparticles.

Chitosan is produced from chitin which can be found as supporting materials in some aquatic and terrestrial organisms as well as in some microorganisms. Chitosan is a

renewable source and natural raw material that is classified as food grade polymer by Food and Drug Administration (FDA). It is classified as biocompatible, biodegradable and nontoxic polysaccharide. Moreover, chitosan is known as an inherently antimicrobial polymer (Janes et al. 2001). Chitosan can form nanoparticles via ionic gelation with small polyanions. Sodium tripolyphosphate is one of the mostly used polyanion to cross-link chitosan. The most important advantage of ionic gelation method is the use of complete hydrophilic environment and mild preparation conditions (Agnihotri et al. 2004). The avoidance of organic solvent usage during preparation is very important especially for edible food packaging that is in direct contact with food.

Another important nanoparticle that has important properties to be used in food packaging is zein nanoparticle (ZNP). Zein is a prolamine which is a characteristic class of proteins and it is the major storage protein of corn and is only soluble in organic solvents such as ethanol. Zein is not appropriate for human consumption due to its negative nitrogen balance and poor solubility in water and also deficiency in essential amino acids which makes it poor in nutritional quality. Zein can be produced in film form and it exhibits toughness, glossy surface and hydrophobicity. Zein is also in the center of commercial interest because of being a renewable source and having potential in many applications (Shukla and Cheryan 2001).

The most important characteristic of zein is insolubility in water except in the presence of alcohol, urea and alkali (pH 11 or above) or anionic detergents. The high proportion of non-polar amino acid residues and deficiency in basic and acidic amino acids is responsible for the insolubility of zein in water (Shukla and Cheryan 2001).

Zein is studied as carrier of active agents as nanobeads or nanoparticles for the purpose of incorporation directly into the food environment. The most important challenge is the dispersion of zein nanoparticles in aqueous food environment. Li et al. (2013) reported a procedure that overcomes this problem by coating zein nanoparticles with sodium caseinate and enable the dispersion of particles in water medium.

CHAPTER 3

MATERIALS AND METHODS

3.1. Materials

Whey protein isolate BiPRO and sodium caseinate were purchased from Davisco Foods and American Casein Company, respectively. Low molecular weight chitosan (molecular weight from 50 to 190 kDa, 75-85% deacetylated), sodium tripolyphosphate pentabasic, corn zein from maize and sodium hydroxide were supplied from Sigma-Aldrich Chemical. Glycerol and acetic acid was used from Panreac. Mueller Hinton agar and ethanol were provided from Merck. Bacteriological peptone was obtained from Oxoid. Deionized water was used for all preparations.

3.2. Preparation of Nanoparticles

3.2.1. Preparation of Chitosan Nanoparticles

Chitosan nanoparticles (CSNP) were prepared by the ionic gelation technique using sodium tripolyphosphate (TPP) as polyanion with procedure adapted from method first reported by Calvo et al. (1997). Commercial chitosan was modified to increase its deacetylation degree before using in nanoparticle preparation. For this purpose, commercial chitosan was first dissolved in 1% (v/v) acetic acid solution overnight. Then, 1 M NaOH solution was dropped slowly in chitosan solution with rapid stirring until pH of the solution was 9.0 to decrease the chain length of chitosan polymer by chain scission. After stirring for four hours, solution was centrifuged (Hettich, Rotina 380 R), rinsed with water and shaken repeatedly to remove NaOH and precipitates were then freeze-dried (Labconco, Freezone 18). Chitosan was then mixed with 1 M NaOH solution again in a water bath (IKA, HBR Digital) at 100°C and 500 rpm for an hour. Washing process was repeated again with centrifuge and water to remove the remaining NaOH in the solution and finally precipitated chitosan was dried at 40°C (Memmert).

For nanoparticle production, 4 mg/ml modified chitosan solution was dissolved in 1% (v/v) acetic acid solution and mixed overnight and 1 mg/ml TPP solution was prepared in water. 25 ml TPP solution was added drop wise at 4 ml/min rate with syringe pump (Goldman) to 25 ml chitosan solution under magnetic stirring to prevent agglomeration. The stirring at room temperature was continued at 500 rpm for two hours. Nanoparticle suspension was then centrifuged at 10000 rpm for 25 min and washed twice to remove free chitosan and TPP in the supernatant of the suspension. Nanoparticle precipitates were re-dispersed in water to add into WPI solution.

3.2.2. Preparation of Zein Nanoparticles

Water soluble zein nanoparticles (ZNP) were prepared by antisolvent precipitation according to the procedure reported in literature (Li et al. 2013). Zein (0.5 g) was dissolved in 80:20 (v/v) ethanol/water solvent. Sodium caseinate (1% w/v) was also dissolved in 250 ml water and poured into zein solution in a second under continuous stirring (1000 rpm). Ethanol was removed by rotary evaporator (Heidolph) and resultant mixture was then centrifuged at 4000 rpm for 10 min to separate large aggregates in mixture prior to freeze-drying. Powdered zein nanoparticles were stored at 4°C until used. ZNP was re-dispersed in water before added into WPI solution.

3.3. Preparation of Chitosan Nanoparticle/Whey Protein Isolate (CSNP/WPI) and Zein Nanoparticle/Whey Protein Isolate (ZNP/WPI) Films

WPI (0.5 g) was dissolved in water to prepare 7% (w/v) solution with magnetic stirrer in natural pH 7. Glycerol was then added to WPI solution as plasticizer (60%, w/w of WPI) and solution was heated at 90°C for 30 minutes in a water bath to denature the protein. Zein nanoparticles were added at ratios of 20, 40, 80 and 120% (w/w of WPI) and chitosan nanoparticles were added at ratios of 2, 6, 12 and 20% (w/w of WPI). Zein and chitosan nanoparticles were re-dispersed in deionized water before adding to WPI solutions. Nanoparticles were added slowly under rapid stirring and mixed overnight to have good dispersion in protein solutions. The film forming solutions were then cast onto polypropylene substrate (8 cm x 8 cm) and dried at 25°C

and 40 ± 1 %RH for 24 hours in an environmental chamber (Angelantoni). Films were easily peeled and stored at room temperature.

3.4. Characterization of Nanoparticles

3.4.1. Dynamic Light Scattering (DLS)

Particle size, particle size distribution and zeta potential were measured with dynamic light scattering (Malvern Instruments, Zetasizer Nano ZS). All measurements were performed in triplicate.

3.4.2. Fourier Transform Infrared (FTIR) Analysis

FTIR analysis was performed on modified chitosan, TPP and CSNP to confirm the formation of nanoparticles. FTIR spectra were obtained with FTIR spectrometer (Perkin-Elmer, Spectrum) in the range of 400 to 4000 cm^{-1} wave number. Samples were mixed with KBr and pressed in dies to obtain pellets. Results were normalized by dividing the absorbance values to maximum absorbance for each spectrum and then plotted to compare.

3.4.3. Scanning Electron Microscope (SEM)

SEM (FEI, Quanta250 FEG) was used to study the morphology and size of the nanoparticles. 3 µl droplet of diluted nanoparticle suspension was dried on double stick carbon tape then coated with gold. All samples were examined using an accelerating beam at voltage of 5 kV.

3.5. Characterization of CSNP/WPI and ZNP/WPI Nanocomposite Films

3.5.1. Film Thickness

Film thickness of prepared films was measured with a digital micrometer (Mitutoyo, 293-821) at five random points for each film sample used in different characterization techniques and mean values were used for further analysis in water vapor permeability and mechanical properties.

3.5.2. Mechanical Properties

The preparations of film specimens and measurements were done according to ASTM D-882-02 standard. Texture analyzer (Texture Technologies, TA.XTPlus) equipped with 5 kgf load cell was used in tensile mode to measure maximum tensile strength, percentage elongation at break and elastic modulus (Young's modulus) of the films from stress-strain curve. Sample films were conditioned at 50% RH and 23°C for 48 h before measurements. Film strips with 5 mm width were mounted on cardboard grips with initial grip separation of 50 mm and test speed was set to 25 mm/min. Tensile strength (TS) was determined as the maximum stress that film could withstand which was calculated by dividing maximum load by initial cross sectional area of the strip. Percent elongation at break (E) was determined as the strain at the fracture point which was the percentage of the ratio of the change of length of the specimen to initial length. Elastic modulus (EM) was calculated from the slope of linear region in stress-strain curve. Measurements were performed at least in seven replicates for each film concentrations and the average of five results was reported.

3.5.3. Water Vapor Permeability (WVP)

Water vapor permeability (Mocon, Permatran-W 3/33 Plus) was measured in accordance with ASTM F 1249-90 standard at 24°C and 25 ± 1 % RH. Specimen areas were fixed to 5 cm^2 and specimens were sealed into the test cell by hydrophobic grease

to prevent air entrance (Figure 3.1). Nitrogen gas (N_2) flow was set to 100 standard cubic centimeters per minute (SCCM) as permeated water vapor carrier gas. Four specimens for each film were analyzed and data were recorded as water vapor transmission rate (WVTR) in g/m^2.day unit. The WVP results (g.mm/m^2.h.kPa) were calculated using Equation 3.1 and 3.2:

$$P_w = S\,(R_1 - R_2) \tag{3.1}$$

$$WVP = \frac{WVTR}{P_w} L_{film} \tag{3.2}$$

where P_w is the water vapor partial pressure gradient across specimen (kPa); S is the water vapor pressure at test temperature (kPa); R_1 is the set relative humidity at outer chamber of the cell (R_1=0.25 for 25%RH); R_2 is the relative humidity of dry N_2 at inner chamber of the cell and L_{film} is the average thickness of the specimen (mm).

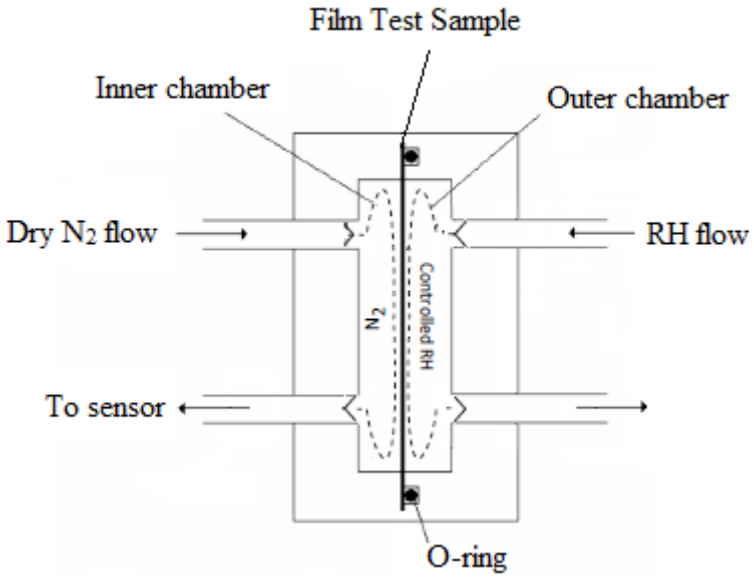

Figure 3.1. Representation of water vapor transmission measurement in test cell

3.5.4. Contact Angle Measurement

Contact angle measurements were performed using optical tensiometer (KSV, Attension Theta) to measure the wettability properties of the films. Measurements were

performed in static mode. A droplet of deionized water (6 µl) was dropped onto the film surface and images of water droplet were recorded in trigger mode. Each measurement was evaluated by taking one frame per second for 5 min. Measurements were performed for pure WPI and films with the highest nanoparticle concentration of ZNP and CSNP at random places of each film surfaces. Changes of contact angle at both sides of the droplet between the baseline of the drop and the tangent at the drop boundary was measured over time with quantification of changes in the droplet shape by the software using Young equation. Wettability properties were further analyzed by evaluating the absorption rate of droplet by the film.

3.5.5. Morphological Properties

3.5.5.1. Scanning Electron Microscope (SEM)

Scanning electron microscope (FEI, Quanta250 FEG) was used to study the morphology of the cross sections of the films. Measurements were performed for pure WPI and films with highest nanoparticle concentration of ZNP and CSNP to observe the dispersions and structural changes within the matrix. Specimens were prepared by fracturing films with liquid nitrogen and mounted on double stick carbon tape to stand in upright position and coated with gold. All samples were examined using an accelerating beam at voltage of 5 kV. Scanning Transmission Electron Microscope (STEM) analysis (FEI, Quanta250 FEG) was further applied to view the dispersed particles in film-forming matrix. Samples were prepared by dropping diluted film-forming solution on the grid and drying. STEM mode of scanning electron microscopy was used.

3.5.5.2. Atomic Force Microscopy (AFM)

AFM analysis (Digital Instruments, MMSPM Nanoscope IV) was used to view the dispersed nanoparticles in WPI matrix. Measurements were performed for pure WPI and films with highest nanoparticle concentration of ZNP and CSNP. Two types of specimens were prepared. Initially, film solutions were diluted to reduce the roughness

at the surface of the film that is in contact with air. 10 µl of droplet was deposited on clean silicon wafer surface to dry and take image of the surface. Second, film-forming solutions were cast on clean glass surface without any dilution. After drying, films were peeled and images of the surface that were in contact with glass was taken. Microscope was operated in tapping mode for all samples. AFM images with scan sizes of 10 x 10, 5 x 5 and 1 x 1 µm were acquired.

3.5.6. Determination of Viscoelastic Properties of Films by Dynamic Mechanical Analysis (DMA)

DMA (TA Instruments, DMAQ800) tests were performed to measure the viscoelastic properties of the films, hence, to find the relationship between barrier and structural properties of the films. Measurements were performed for pure WPI and films with the highest nanoparticle concentration of ZNP and CSNP to compare and comment on the effect of nanoparticle addition on the structure. Film strips were cut in 35 mm length and 5 mm width; mounted on tension film clamps and coated with hydrophobic grease. Measurements were performed in temperature ramp mode from -60°C to 25°C with heating rate of 3°C/min at 10 Hz. Storage modulus and loss modulus curves were recorded with increasing temperature.

3.5.7. Differential Scanning Calorimetry (DSC)

DSC (TA Instruments, Q10) tests were performed to observe the changes in the crystallinity of the films upon nanoparticle addition. Measurements were performed for pure WPI film and the films obtained with the highest nanoparticle loadings. Films weighed around 6.5 mg in aluminum pan were exposed to 50 ml/min nitrogen gas and temperature was increased from 0°C to 220°C with a 5°C/min ramp. Heat flow curves were recorded with increasing temperature.

3.5.8. Antibacterial Test

Antibacterial properties of pure WPI films, CSNP/WPI and ZNP/WPI films with highest nanoparticle concentrations were analyzed by disc diffusion method. Mueller-Hinton agar (MHA) and bacteriological peptone water were prepared and autoclaved at 121°C for 15 min. Then, MHA were poured in petri dishes and held in incubator over night at 37°C to check the sterilization. *E.Coli* (ATCC 25922) were spread on MHA and incubated for 24 h at 37°C. *E.Coli* was then adjusted to 0.5 McFarland in 10 ml peptone water and spread on MHA by swab at three different angles. Three samples for each film were then cut in 17 mm diameter and both surfaces of the films were sterilized under UV radiation for one min. Samples were then put on agar surfaces coated by bacteria and held at incubator for 24 h at 37°C.

CHAPTER 4

RESULTS AND DISCUSSION

4.1. Characterization of Nanoparticles

4.1.1. Modification of Chitosan

Chitosan (CS) is the deacetylated form of chitin which is a cationic amino polysaccharide copolymer of N-acetyl-D-glucosamine and D-glucosamine units linked with β-(1-4) glycosidic bond (Figure 4.1) (Kim 2011). The term chitosan is used for both partially and completely deacetylated chitosan. However, completely deacetylated chitosan is not commercially available (Kasaai 2011). Therefore, deacetylation degree (DD) of commercial chitosan is always indicated in its properties. Commercial chitosan has molecular weight ranging between 3800 and 20000 Dalton and deacetylation degree ranging between 66 and 95% (Agnihotri et al. 2004).

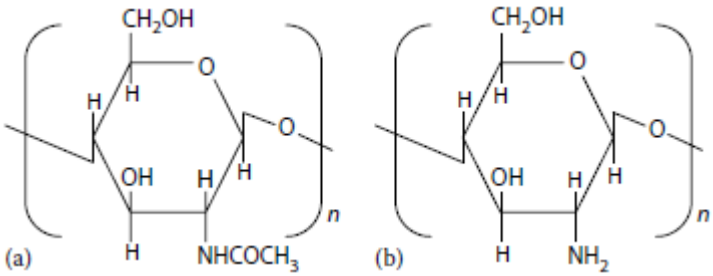

Figure 4.1. Chemical structures of (a) chitin and (b) chitosan
(Source: Kim 2011)

In neutral or basic pH conditions, CS (isoelectric point around 6.5) is insoluble in water due to free amine functional groups. When amine groups get protonated in acidic conditions, it becomes soluble and tends to form hydrogels with polyanions which mediate inter- or intramolecular cross-linking (Janes et al. 2001; Grenha 2012; Agnihotri et al. 2004). In this study, chitosan nanoparticles (CSNP) were obtained with ionic gelation between cationic CS and polyanionic sodium tripolyphosphate (TPP).

Formation of CSNP is based on electrostatic interaction between positively charged amine groups of CS and negatively charged phosphate groups of TPP.

CSNP formation strongly depends on amount of amine groups which is mainly determined by deacetylation degree (DD) of CS. In literature, it was observed that DD and molecular weight of CS can be controlled by alkali treatments. Zhang et al. (2004) reported that increasing deacetylation degree of chitosan and modifying its molecular weight distribution by fractionation and deacetylation steps caused decreased particle size and polydispersity index (PDI) indicating formation of monodispersed nanoparticles. Increased deacetylation led to formation of more positive charged sites on CS and higher degree of cross-linking with TPP. As a result, denser and smaller CSNP were obtained.

In this study, commercial CS (CCS) was initially modified with a technique adapted from the study of Zhang et al. (2004) in order to increase its DD and decrease the polymer chains to obtain nanoparticles with a narrow size distribution, denser and more compact structure. To achieve better NP size control, first molecular weight distribution of CCS was narrowed by fractionation through dropwise addition of alkaline solution under severe mixing. Addition of NaOH solution into chitosan resulted in chain scission of the backbone and generated shorter chains than the unmodified CS (Kasaai 2011). It is reported that, shorter chains penetrate easily into partially formed CS-TPP leading to smaller and denser nanoparticles. Second, increasing deacetylation degree (DD) was aimed by heating fractionated CS with alkaline solution to convert the amide group to amine groups. Hydroxyl ions in NaOH solution attack to carbon of the carbonyl groups and amide group convert to amine groups upon hydrolysis. This leads to increased positively charged groups in acidic conditions and cross-linking of amine groups which would result in more compact structure.

Table 4.1. Important bond in FTIR spectra of commercial CS (CCS) and fractionated and deacetylated CS (FDCS) with corresponding wave number

Wave number (cm^{-1})	**Bond**
1690-1630	C=O stretch (amide I)

The change in the degree of deacetylation of commercial chitosan through modification was characterized with FTIR analysis which is a relatively easy method for a qualitative evaluation. FTIR spectra of both commercial chitosan (CCS) and

fractionated and deacetylated chitosan (FDCS) are seen in Figure 4.2. Important spectral regions are at 1650-1750 cm^{-1} which represent carbonyl groups (-C=O) in amide band (Table 4.1). Results showed that absorbance of amide I bond at 1655 cm^{-1} of CCS was stronger than the absorbance of FDCS and intensity apparently reduced which indicates an increase in DD of commercial chitosan. These results are in good agreement with the findings of Zhang et al. (2004).

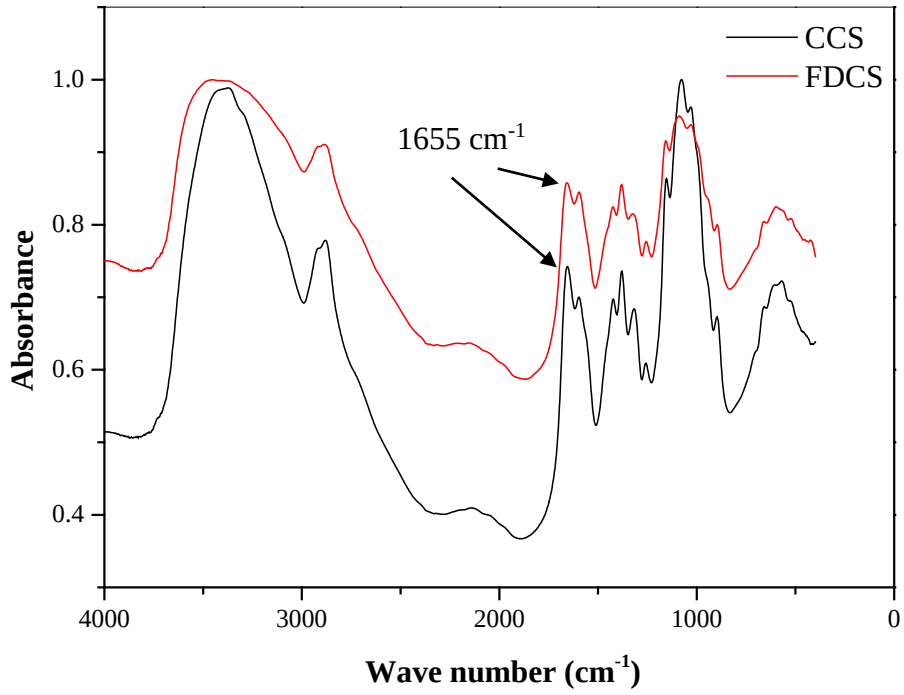

Figure 4.2. FTIR spectra of commercial CS (CCS) and fractionated and deacetylated CS (FDCS)

4.1.2. Particle Size and Zeta Potential of Chitosan (CSNP) and Zein Nanoparticles (ZNP)

Particle size, polydispersity index (PDI) and zeta potential of CSNP and ZNP measured with dynamic light scattering are presented in Table 4.2. Particle sizes of nanoparticles are reported based on number weighted distributions. Mean sizes of the nanoparticles were 62 ± 2 and 77 ± 1 nm for CSNP and ZNP, respectively. Monodisperse size distribution was observed for each nanoparticle with polydispersity indexes smaller than 0.5 (Figure 4.3 and Figure 4.4). In addition, overlapping of the three peaks for each nanoparticle also indicated that there were no agglomeration in

nanoparticle dispersion during the measurement confirming proper sample preparation. Chitosan nanoparticles synthesized from unmodified commercial chitosan was larger with a mean size of 88 ± 33 nm and had a higher polydispersity index (PDI=0.55) than the CSNPs obtained from fractionated and deacetylated chitosan. This result simply indicates the importance of modifying the commercial chitosan to have a better control on the size and size distribution of CSNP. Polydispersity index of zein nanoparticles was found to be lower than chitosan nanoparticles. Particle sizes were also evaluated in SEM images to compare with the results of DLS.

Zeta potentials of CSNP and ZNP were found to be +30 mV and -40.91 mV for CSNP and ZNP, respectively. These results were obtained by dispersing nanoparticles in water with pH similar to pH of the nanoparticle added WPI film forming solution. Opposite charges of nanoparticles would act different in WPI solution which would also affect the final properties of the films.

Table 4.2. Particle size, polydispersity index (PDI) and zeta potential of CSNP and ZNP

	Particle Size (nm)	**PDI**	**Zeta Potential (mV)**
CSNP	62 ± 2	0.376 ± 0.014	30.07 ± 0.80
ZNP	77 ± 1	0.138 ± 0.003	-40.91 ± 1.51

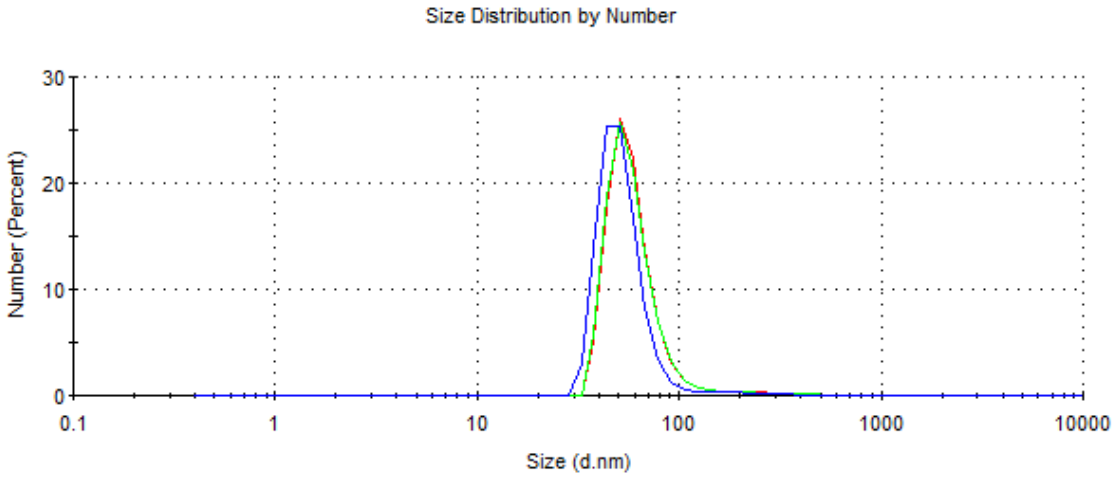

Figure 4.3. Size distribution of CSNP produced with modified chitosan

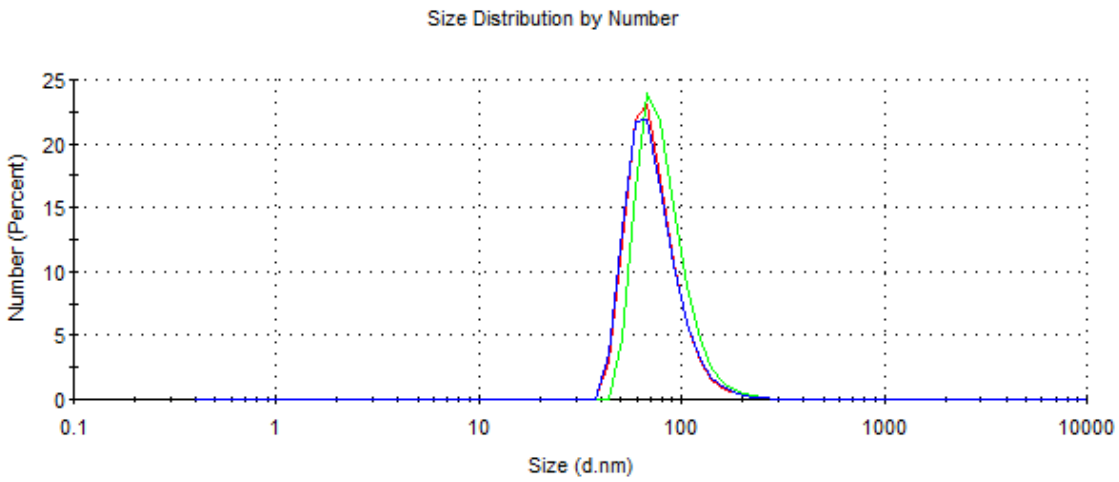

Figure 4.4. Size distribution of ZNP

4.1.3. Formation and Morphology of Nanoparticles

Formation of CSNP was as shown in Figure 4.5. When CS dissolves in aqueous acetic acid, amino groups protonate and form $-NH_3^+$ sites. In the complexation of CS with TPP, positively charged amino group of CS and negatively charged counterion of TPP interacts ionically. At basic pH, TPP releases $P_3O_{10}^{5-}$ ions at high concentrations as well as OH^- ions when dissociated in water. As a consequence, both OH^- and $P_3O_{10}^{5-}$ ions exist in TPP solution. These OH^- and $P_3O_{10}^{5-}$ ions both interact with $-NH_3^+$ in CS by deprotonation or ionic crosslinking, respectively. Both ions can compete to form CS beads by reacting with protonated amino group of CS on the surface of the beads (Figure 4.6). When TPP is dropped in CS solution, spherical gel nanoparticles form immediately by ionotropic gelation. Meanwhile, acetic acid is neutralized by OH^- in CS droplets and diffuses out of droplets. When outer layer forms, due to the smaller size of OH^- ions, they can diffuse into the matrix through gelled film layer easier than $P_3O_{10}^{5-}$ ions. Then, coacervation phase inversion mechanism involves gradually in the gelation of chitosan which is resulted from neutralization of protonated amino group of CS by OH^- ions. (Mi et al. 1999; Fan et al. 2012). As a result, CS is formed by ionic gelation and precipitates to form spherical particles (Figure 4.6).

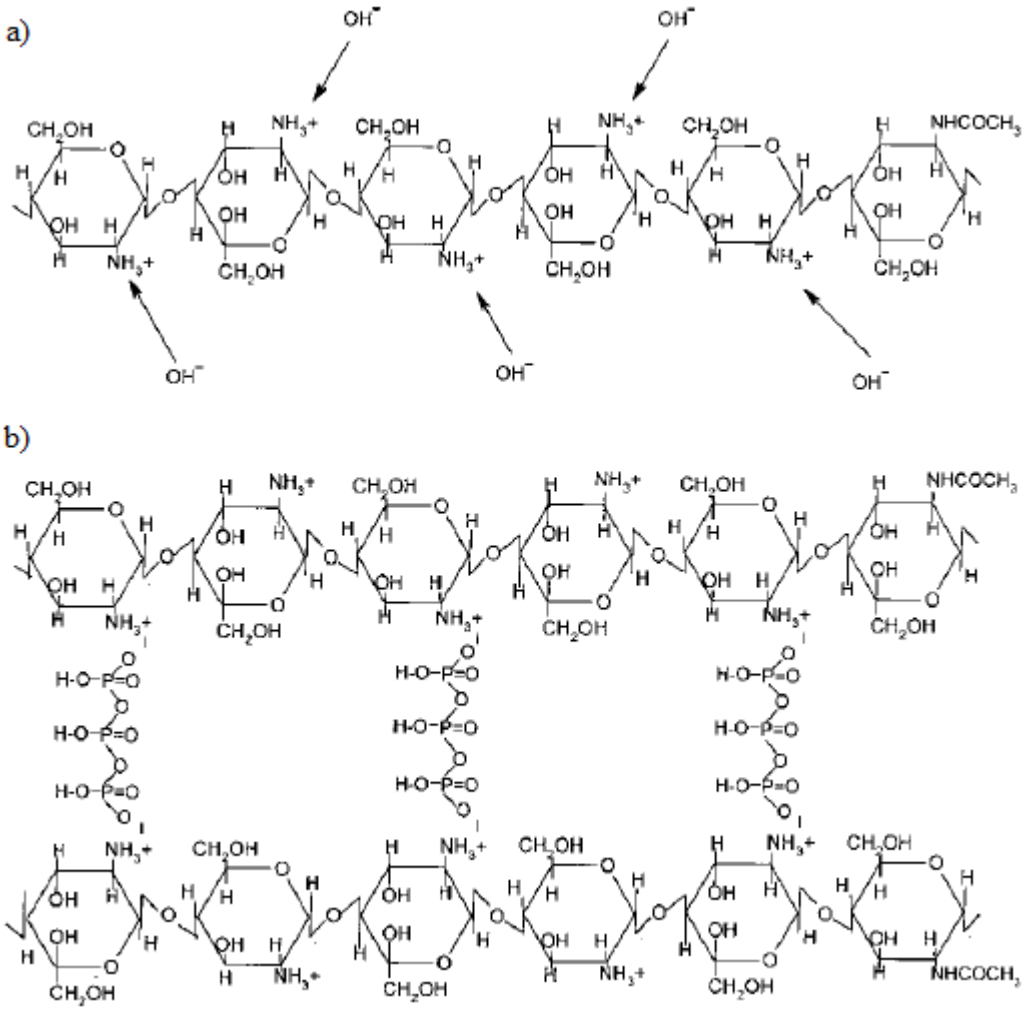

Figure 4.5. Interaction of CS with aqueous TPP a) deprotonation b) ionic crosslinking (Source: Mi et al. 1999)

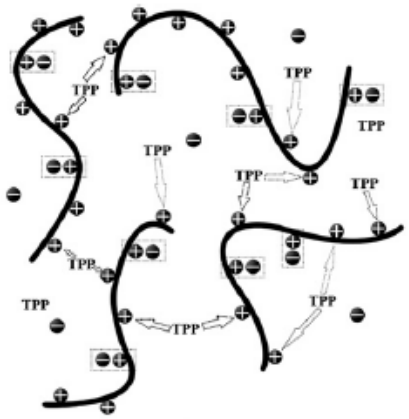

Figure 4.6. Representative illustration of ionic crosslinking between CS and TPP (Source: Fan et al. 2012)

FTIR analysis was performed to determine the formation of CSNP by comparing FTIR spectra of nanoparticles (red line) and fractionated and deacetylated chitosan (black line) (Figure 4.7).

Table 4.3. Important bonds in FTIR spectra of CSNP and FDCS with corresponding wave numbers

Wave number (cm^{-1})	Bond
1690-1630	C=O stretch (amide)
1650-1580	N-H bend (amine)
1320-1140	P = O stretch

In the spectra of CSNPs, peak at 1650 cm^{-1} was shifted and a new sharp peak appeared at 1630 cm^{-1}. Peak of $–NH_2$ band at 1595 cm^{-1} was also shifted to 1539 cm^{-1} indicating that amine groups were involved in cross linking by phosphate groups of TPP (Wu et al. 2005; Dudhani and Kosaraju 2010). In addition, absorption peak occurred at 1225 cm^{-1} which confirmed the P=O stretching (Dudhani and Kosaraju 2010). Thus, these characteristic peaks indicated the formation of nanoparticles.

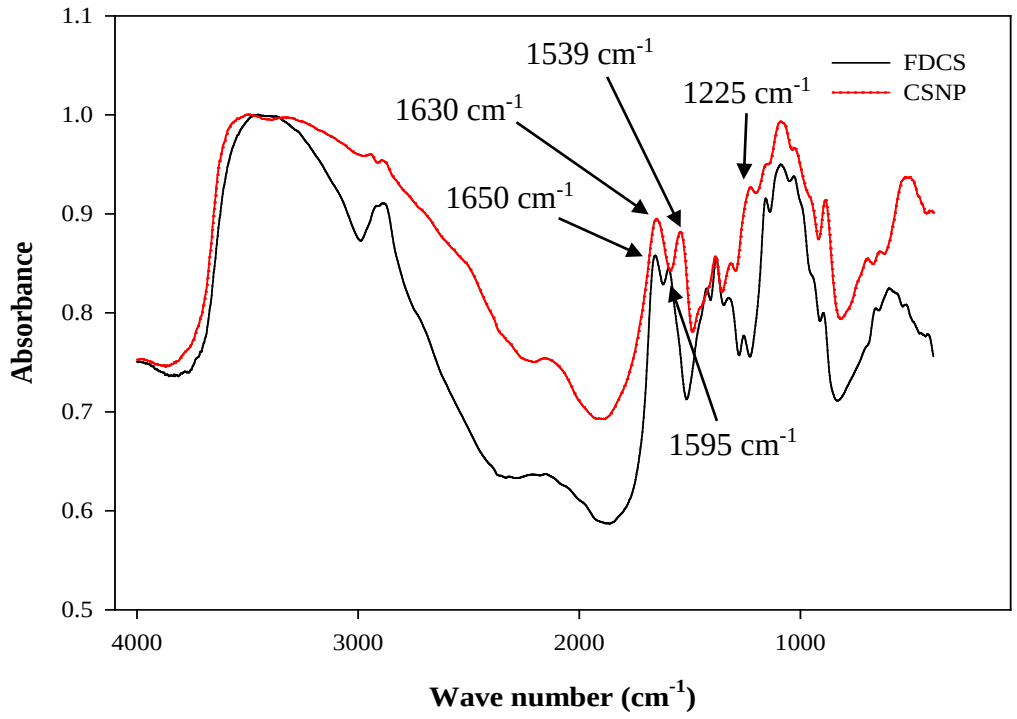

Figure 4.7. FTIR spectra of chitosan nanoparticles (CSNP) and fractionated and deacetylated chitosan (FDCS)

SEM images of CSNP are presented in Figure 4.8. The shape of the particles was observed as spherical and due to agglomerations, nanoparticle clusters were imaged instead of individual nanoparticles. From the images, nanoparticle sizes measured at different points were found in the range of 50-109 nm which is consistent with the size measurements obtained from DLS. SEM samples were prepared by diluting nanoparticle solution several times to be able to take images of individual nanoparticle. However, nanoparticles aggregated and formed a film layer when dried leading to measure wide range of sizes and prevented to take image of the nanoparticles at different areas on the tape.

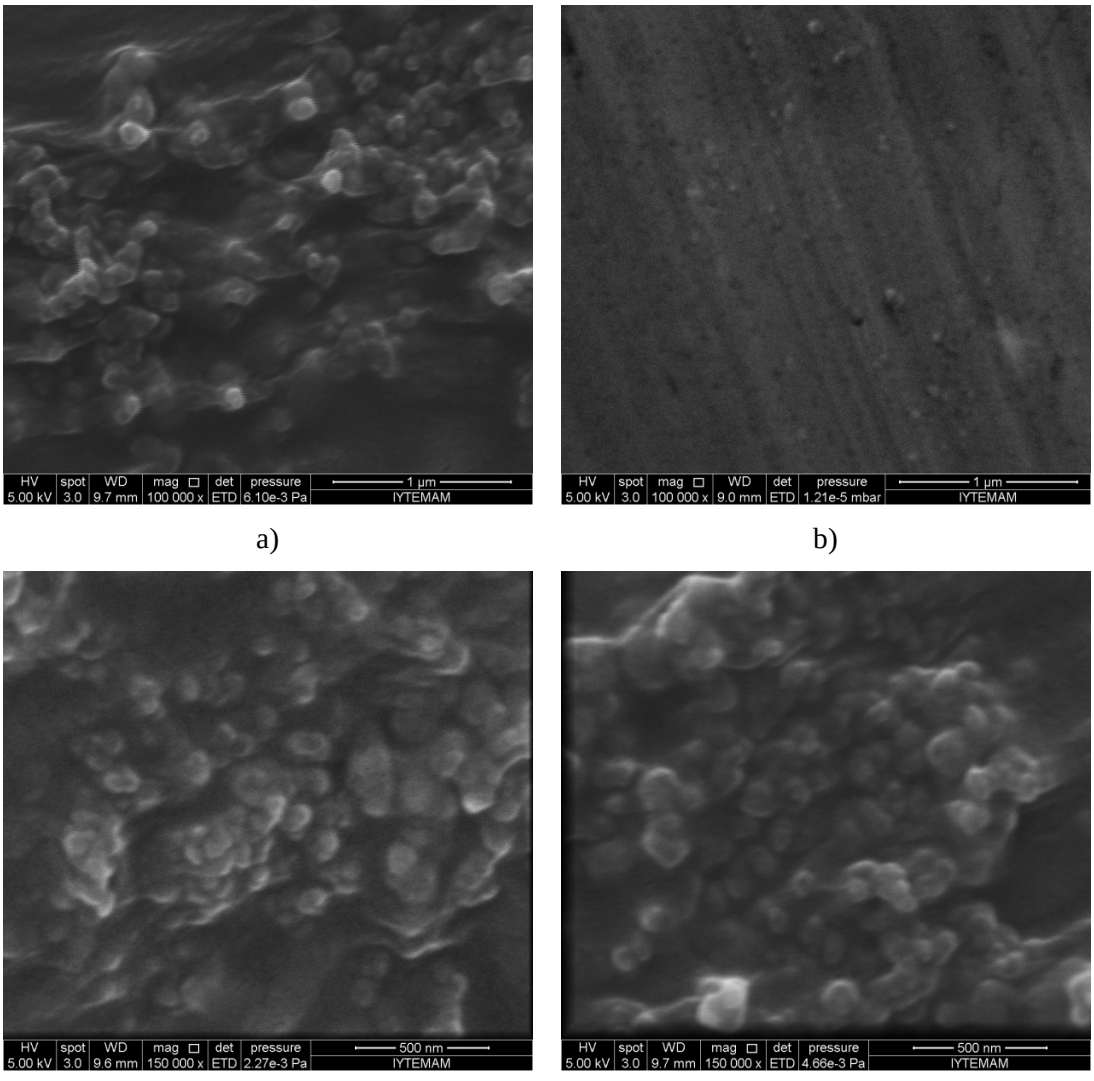

Figure 4.8. SEM images of CSNP a-b)100000 x and c-d) 150000 x

Zein is a hydrophobic biopolymer resulting in hydrophobic nanoparticles which could not be dispersed in water medium due to agglomerations and lead to incorrect measurements in DLS. In order to enable its dispersion in water, zein nanoparticles were produced in the presence of sodium caseinate (SC) by the method adapted from the literature (Li et al. 2013). The formation occurs by strong electrostatic attraction between positively charged zein and negatively charged SC during precipitation process (Patel et al. 2010). The negative zeta potential value shown in Table 4.2 confirmed the wrapping of ZNPs with SC.

SEM images of zein nanoparticles are presented in Figure 4.9. Zein nanoparticles were also spherical in shape and individual particles were clearly observed in images although local gatherings were also encountered. Particle sizes of individual nanoparticles were measured at several points and exhibited variation between 70-160 nm. Number averaged size value obtained from DLS was consistent with the sizes detected from the images.

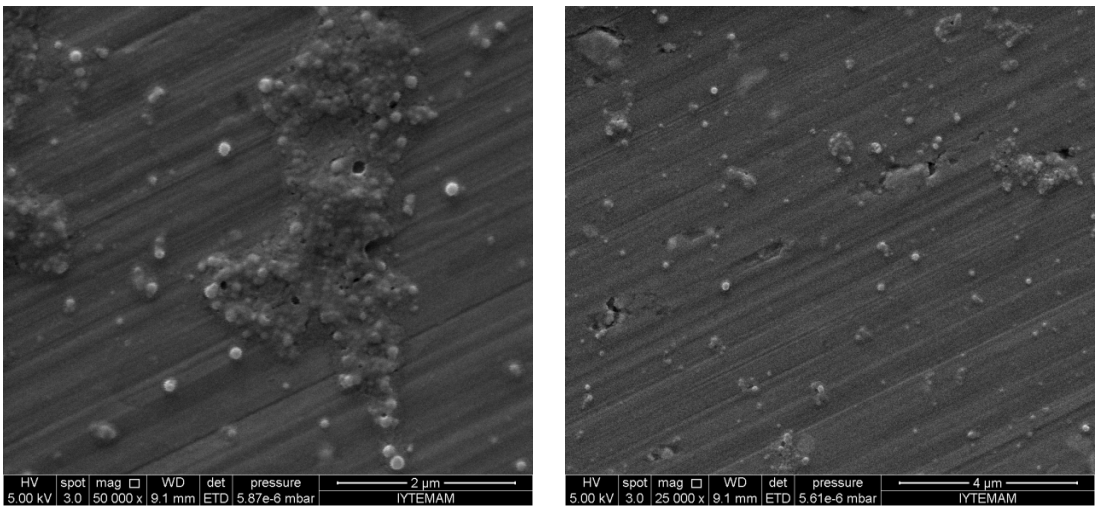

a) b)

Figure 4.9. SEM images of ZNP a) 50000 x b) 25000 x c) 100000 x and d) 25000 x

(cont. on next page)

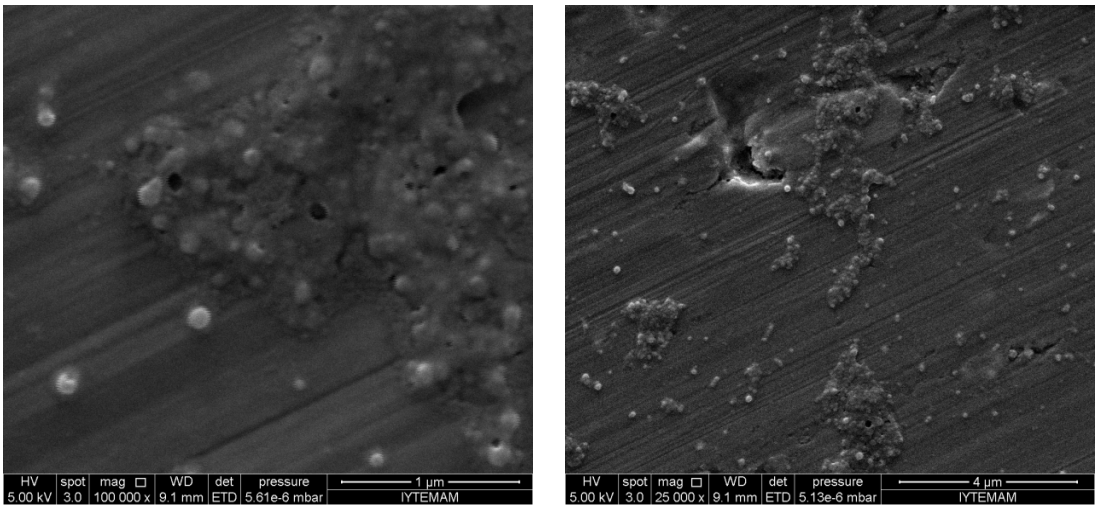

c) d)

Figure 4.9. (cont.)

4.2. Characterization of CSNP/WPI and ZNP/WPI Nanocomposite Films

4.2.1. Morphological Properties

Morphology of the films was characterized by SEM, AFM and STEM measurements in order to observe the dispersion of nanoparticles within the matrix and changes in the structure. Visually, it was observed that pure WPI films were transparent whereas nanoparticle loaded films became translucent.

Cross sectional SEM images of pure WPI and CSNP/WPI films can be seen in Figure 4.10. The cross section of pure WPI film was smooth, nonporous and homogeneous while different morphology was observed all along the cross-section of the CSNP/WPI nanocomposite films indicating the presence of nanoparticles distributed without any phase separation. On the other hand, agglomerations were seen locally and neither the dispersion of particles nor the individual particles were not clearly observed.

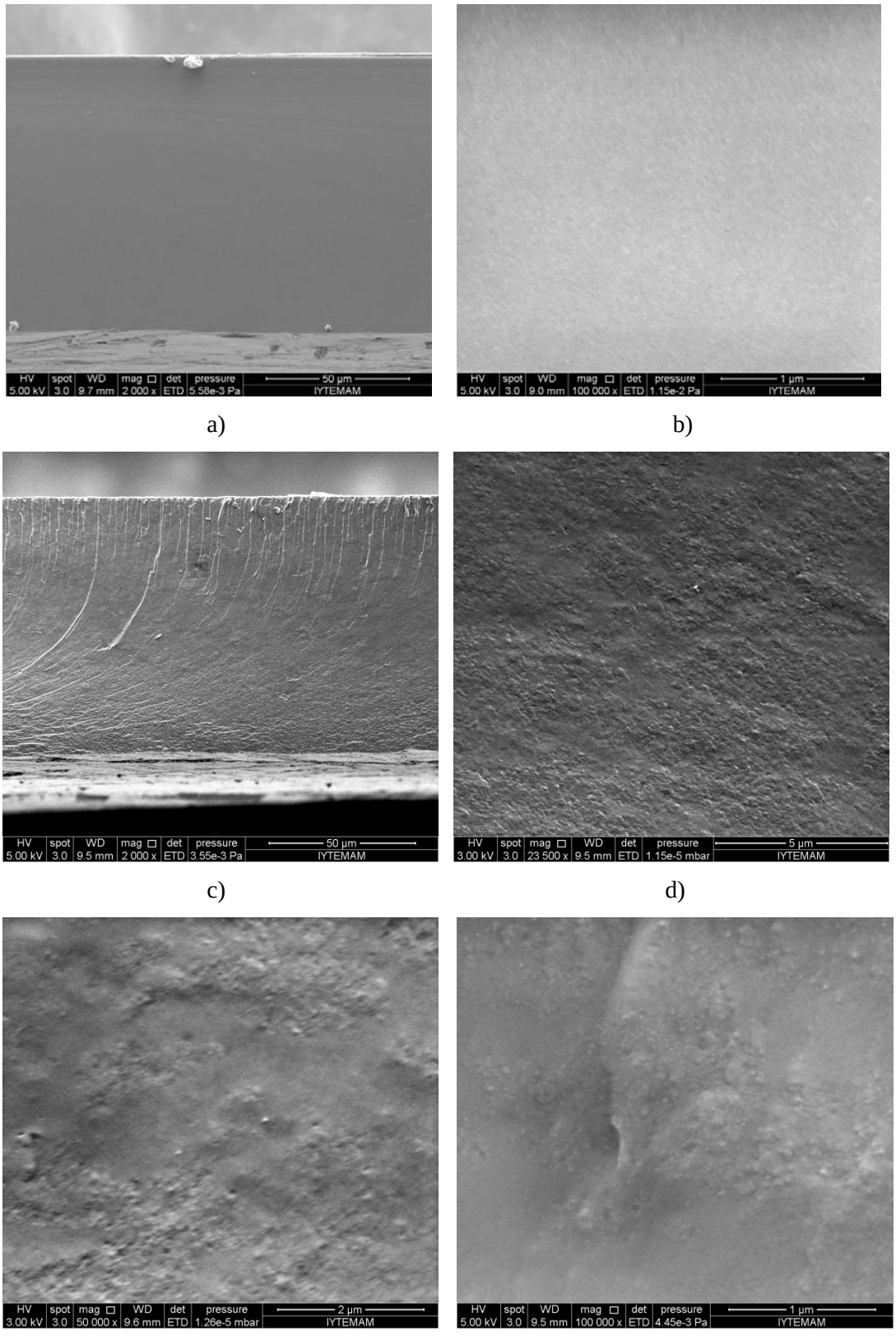

Figure 4.10. SEM images of the cross sections of pure WPI film (a: 2000 x; b: 100000x) and CSNP/WPI films (c: 2000 x; d: 23500 x; e: 50000 x and f: 100000 x)

AFM analysis was also applied to better understand the microstructure of the films. To take the images of the surface that is in contact with air (air side), film forming solutions were diluted prior to drying. Otherwise, measurements failed due to the roughness of the surface. Moreover, images of the surface that were in contact with glass substrate were also taken to evaluate the surface properties and better understand the phases in film composition. These images will be abbreviated as substrate-side.

AFM phase images of pure WPI films are seen in Figure 4.11. Homogeneous structure of WPI films was also confirmed by AFM images. Moreover, globular microstructure of WPI was clearly observed at higher magnifications as reported in literature (Ikeda and Morris 2002) and local aggregations observed probably occurred during heat denaturation of proteins. Small differences between phases were seen from the images which could be attributed to mixed composition of WPI itself due to presence of more than one type of protein.

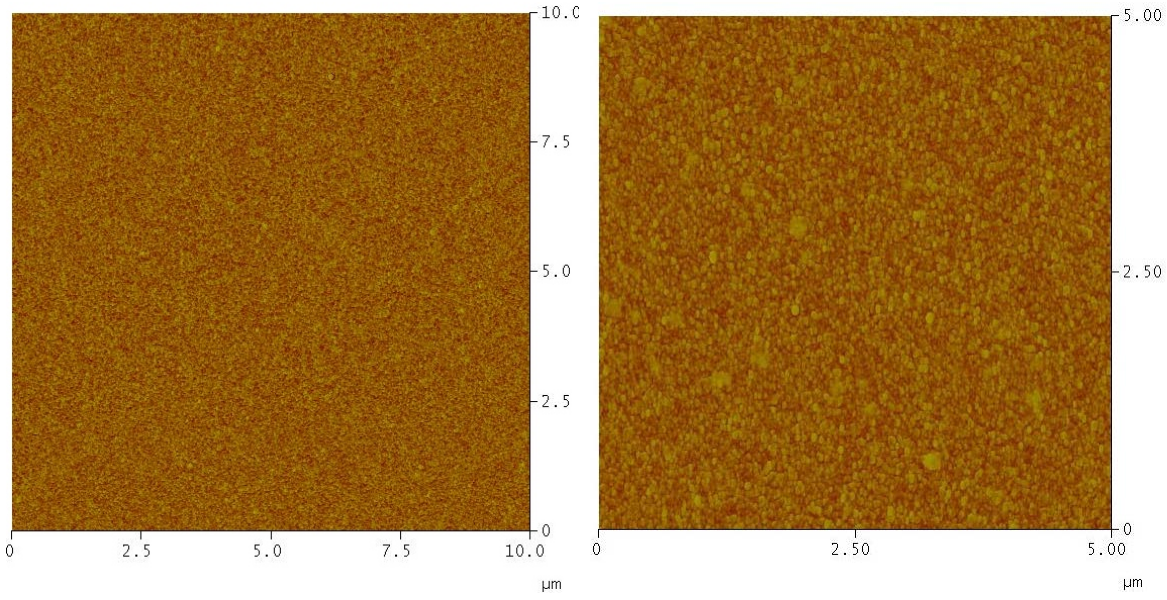

a) b)

Figure 4.11. AFM phase images of pure WPI films a) 10x10 µm- air side; b) 5x5 µm- air side; c) 5x5 µm- substrate side and d) 1x1 µm-air side

(cont. on next page)

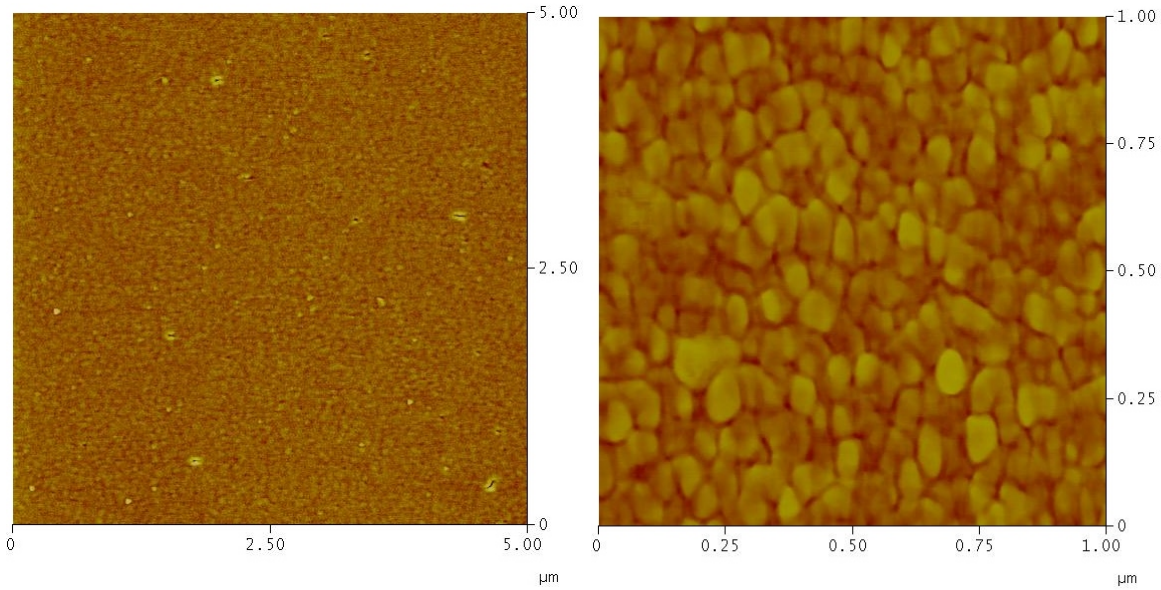

c) d)

Figure 4.11. (cont.)

AFM images of 20% CSNP loaded WPI films were presented in Figure 4.12. CSNP/WPI nanocomposite films showed similar structure to pure WPI with slight differences on the air side images. It was not possible to clearly image CSNPs in Figures 4.12a through 4.12c. In order to observe nanoparticles, the film solution was not diluted and the image was taken from the surface which was in contact with the substrate since drying does not influence the roughness of that surface. Compared to the phase images of substrate side of the pure WPI film, nanoparticles were distinguished as different phase within the matrix. It was clearly seen that nanoparticles were dispersed as closely packed structures in protein matrix as shown in Figure 4.12d through Figure 4.12f.

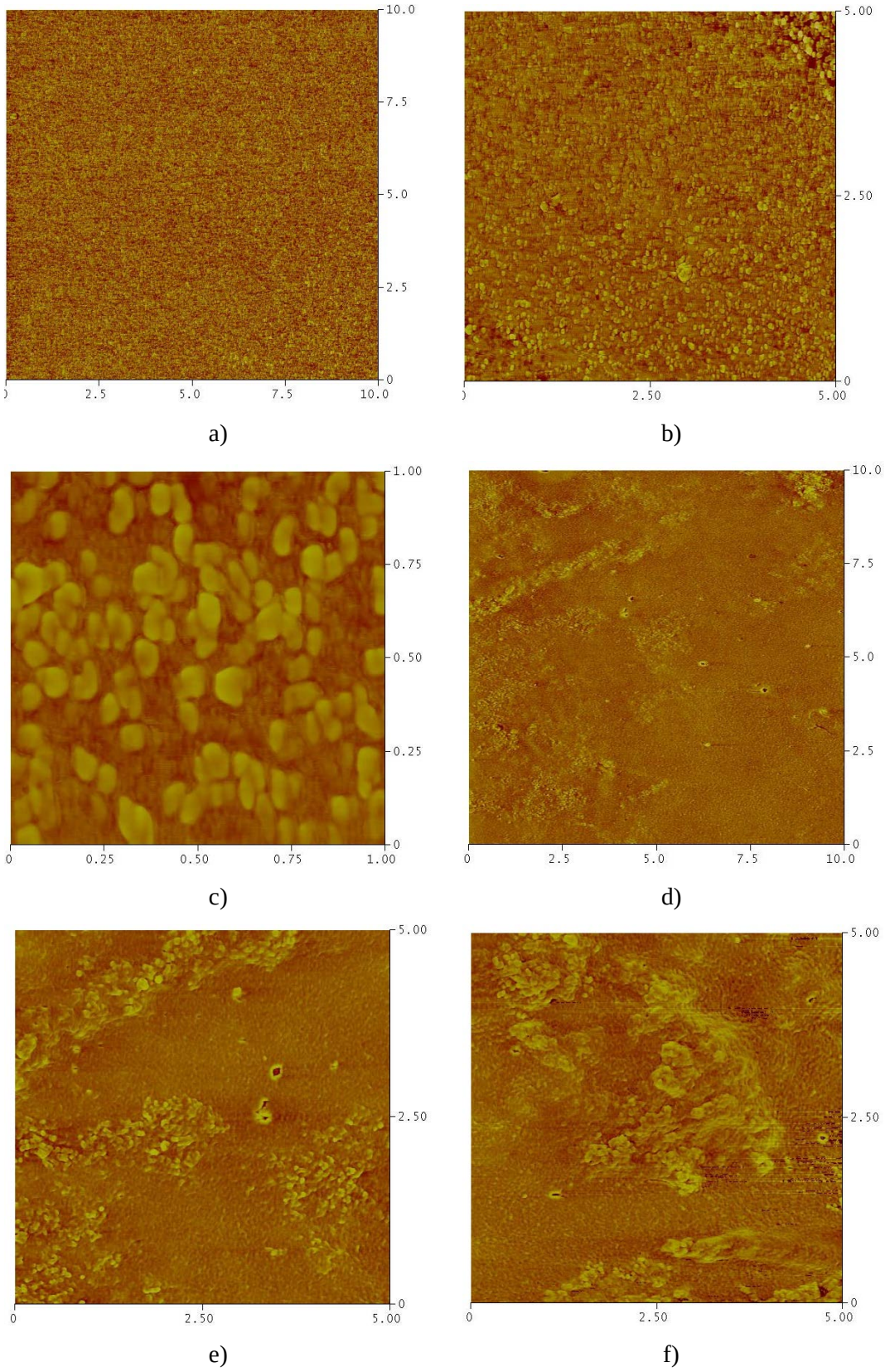

Figure 4.12. AFM images of 20% CSNP loaded WPI film a) 10x10 µm-air side, b) 5x5 µm-air side, c) 1x1 µm-air side, d) 10x10 µm- substrate side, e) 5x5 µm-substrate side and f) 5x5 µm- substrate side

To see the dispersion of CSNPs in bulk matrix rather than the surface, STEM imaging was also studied on CSNP/WPI film. CSNPs were clearly observed as dispersed small white dots in cloudy protein matrix (Figure 4.13). Porosity in the first image belongs to polymeric membrane on the mesh of STEM grid. Again, particle clusters were encountered at different parts of the sample, confirming the results of AFM and tendency to particle agglomeration.

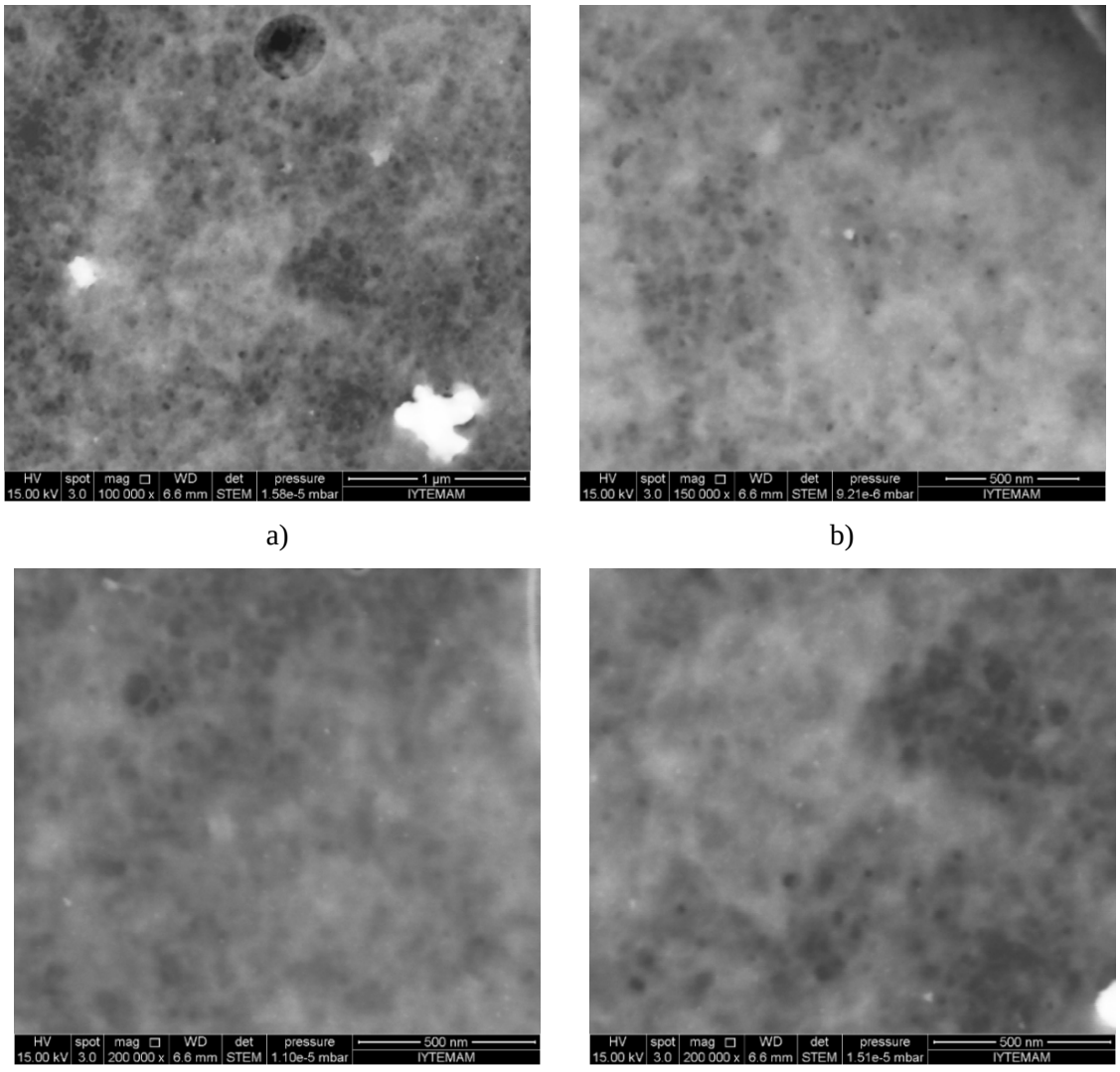

a) b)

c) d)

Figure 4.13. STEM images of diluted 20% CSNP/WPI film a)100000x; b) 150000x; c) and d) 200000x

SEM images of the cross sections of pure WPI and 120% ZNP/WPI films are seen in Figure 4.14. Nanoparticles were clearly seen as scattered individually in the matrix and no agglomerations were encountered. It was also observed that distribution

was homogeneous. Small holes in the images were the traces of nanoparticles that remained on the other side of the film during fracture. Cross sections of the films were prepared by fracturing with liquid nitrogen which prevented any deformation at the interface and nanoparticles were clearly viewed.

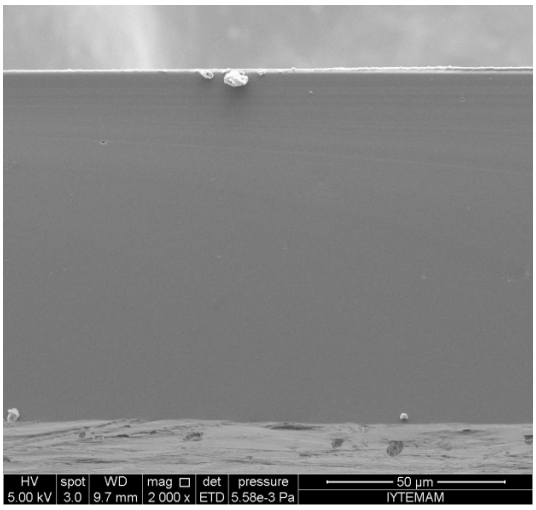

a)

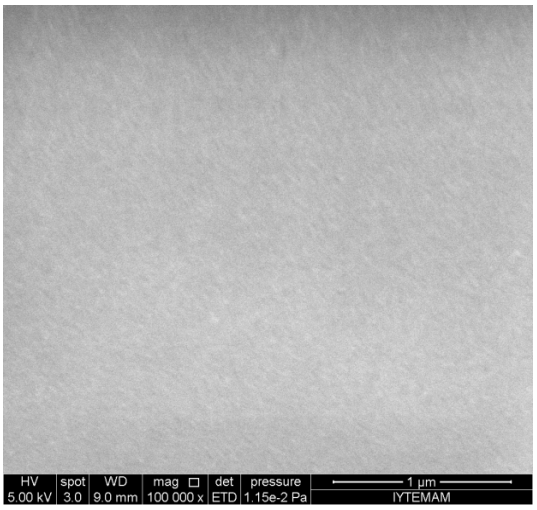

b)

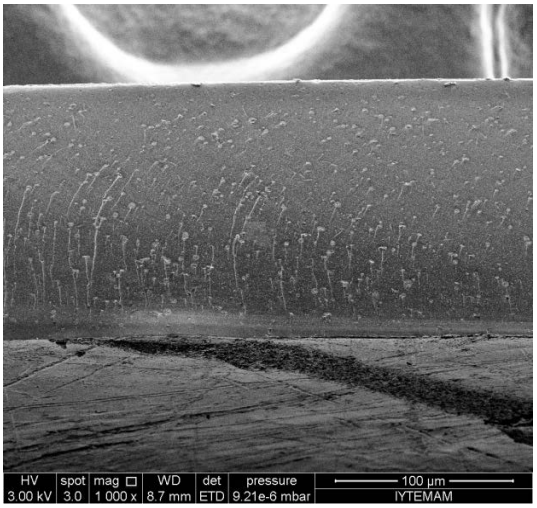

c)

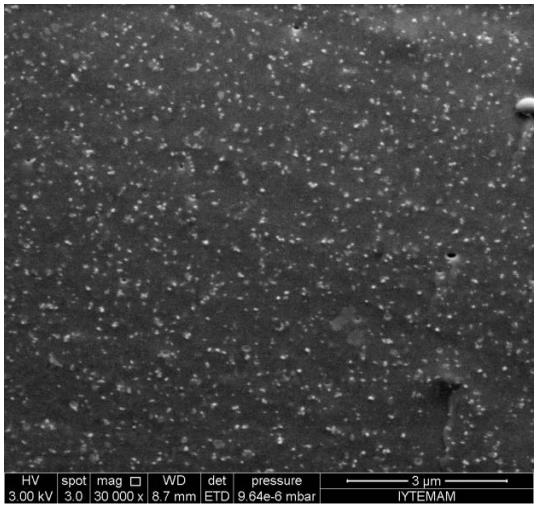

d)

Figure 4.14. SEM images of the cross sections of pure WPI film (a: 2000x; b: 100000x) and 120%ZNP/WPI film (c: 1000 x; d: 30000 x; e: 35000 x; f: 100000 x)

(cont. on next page)

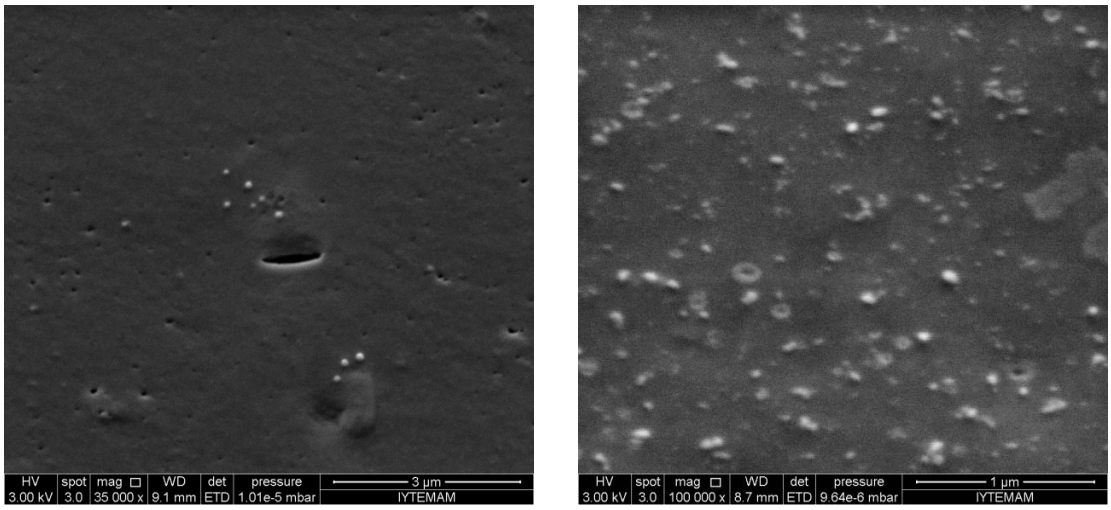

e) f)

Figure 4.14. (cont.)

Homogeneous distribution of zein nanoparticles was also confirmed in the AFM images of ZNP loaded WPI films as can be seen in Figure 4.15. Nanoparticles were viewed individually and phase differences between WPI matrix and ZNP was clearly distinguished.

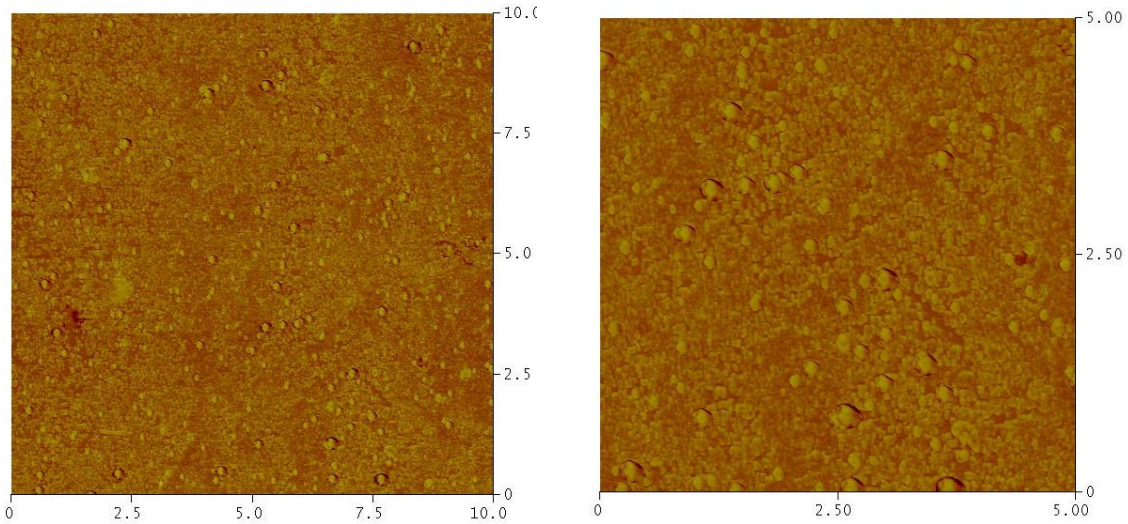

a) b)

Figure 4.15. AFM images of 120% ZNP loaded WPI film a) 10x10 µm-air side, b) 5x5 µm-air side, c) 1x1 µm-air side, d) 5x5 µm-air side e) 1x1 µm-air side

(cont. on next page)

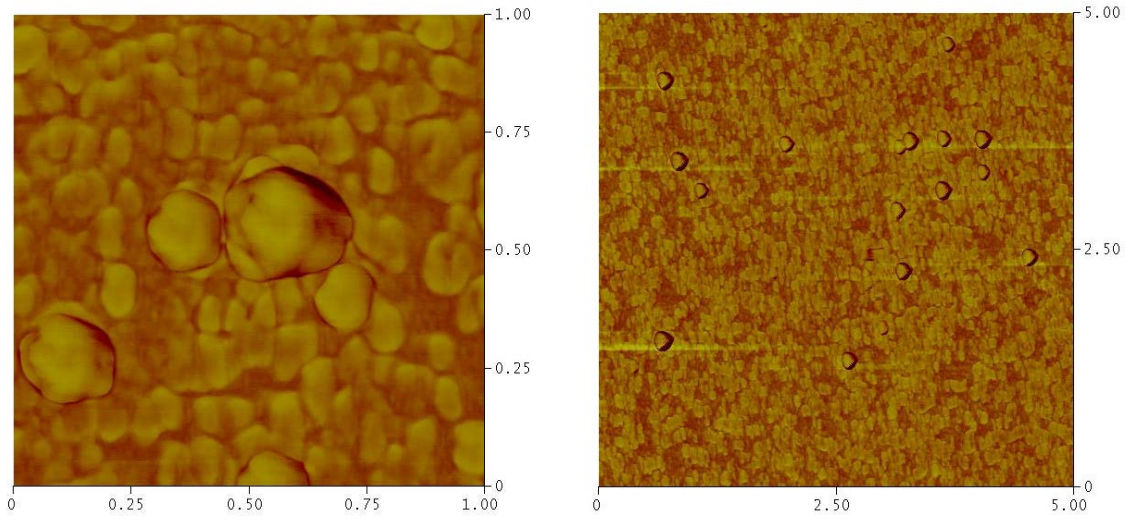

c) d)

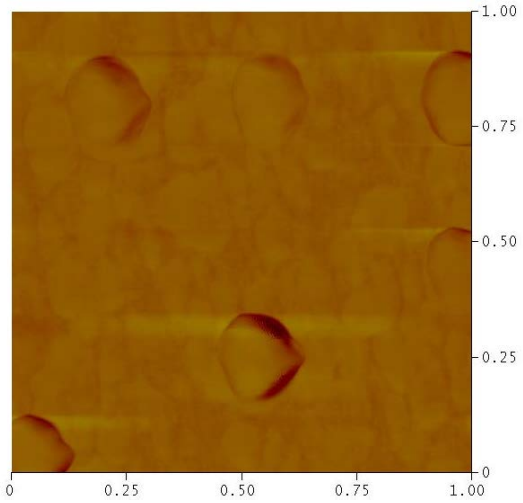

e)

Figure 4.15. (cont.)

The difference in the distribution of CSNPs and ZNPs can be explained by their charge distributions in final film forming solutions. pH of the CSNP/WPI solution was around 6.35 and at this pH, WPI is negatively and CSNP are positively charged which resulted in closely spaced structure due to attractive forces and some agglomerations were clearly seen in images. Homogeneous dispersion of ZNPs can be mainly attributed to repulsive force between negatively charged WPI and ZNP at pH 6.6 of the ZNP/WPI film forming solution.

4.2.2. Mechanical Properties

Mechanical properties of packaging films are important to maintain their integrity during storage and handling. Tensile strength, elongation at break and elastic modulus are parameters that describe the behavior of film under different circumstances and reveal the changes in microstructure of the film.

The effect of CSNP and ZNP loading on the tensile strength (TS) of WPI films are presented in Figure 4.16 and Figure 4.17, respectively. It was observed that TS of the films increased significantly as nanoparticle concentration increased. CSNP incorporation increased the TS of pure WPI film by 160% at highest loading level (20%) and reached to 6.59 MPa. On the other hand, ZNP incorporation increased TS of pure WPI by 303% at highest loading level of 120% to 10.21 MPa. At the same loading level (20%), CSNP increased TS by 106% more than ZNP which can be contributed to attractive interaction between CSNP and WPI. Closer interaction allowed higher strength due to constraining effect to chain movements and increased the strength of the polymer against applied stress.

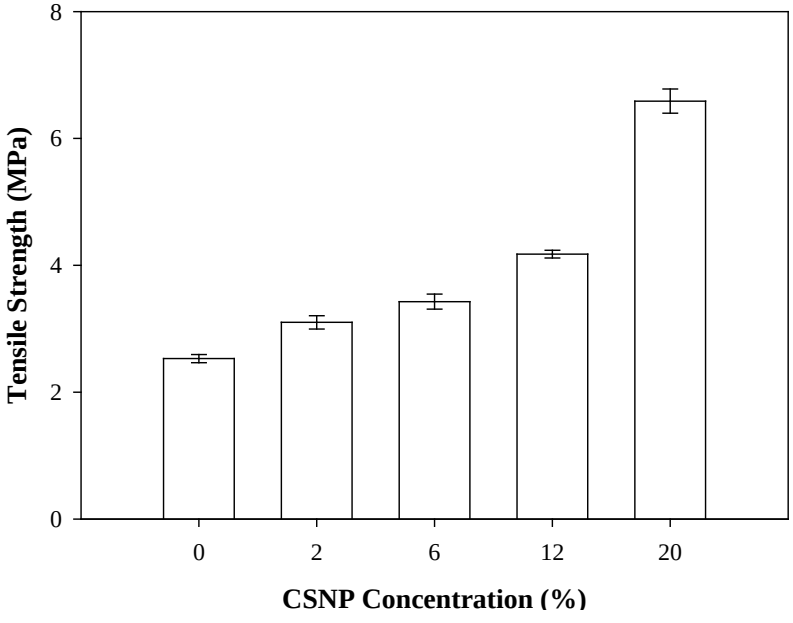

Figure 4.16. Tensile strength results of WPI films incorporated at different ratios

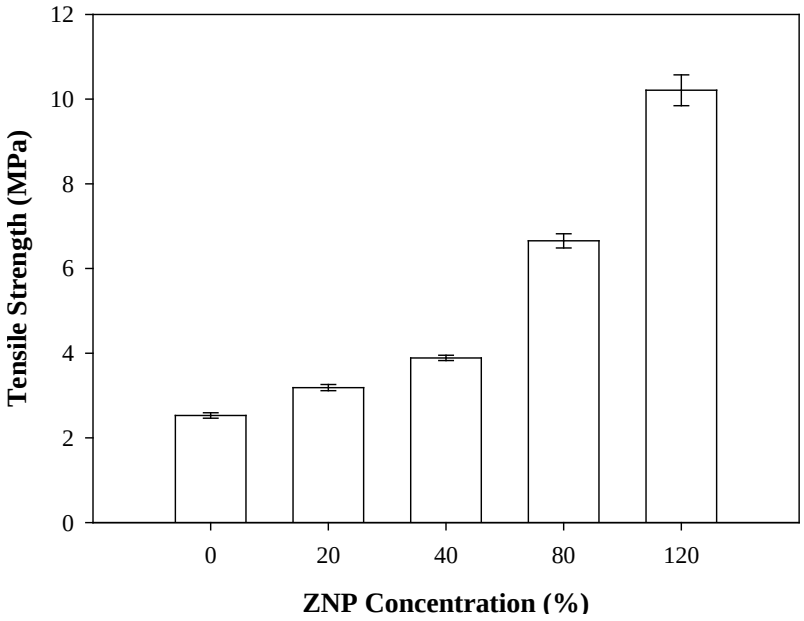

Figure 4.17. Tensile strength of ZNP loaded WPI films at different concentrations

The CSNP loading did not significantly affect the elongation of the film (Figure 4.18) while incorporation of ZNP at the highest loading (120%) slightly decreased the elongation (Figure 4.19). At 20% loading, ZNP acted as a plasticizer, increased the spacing between the chains and mobility of the chains by mitigating the effect of interactions and introduced more free volume in the structure. However, with the increased nanoparticle concentration, antiplasticization effect was observed. Consequently, chains were constrained by nanoparticles and elongation decreased again.

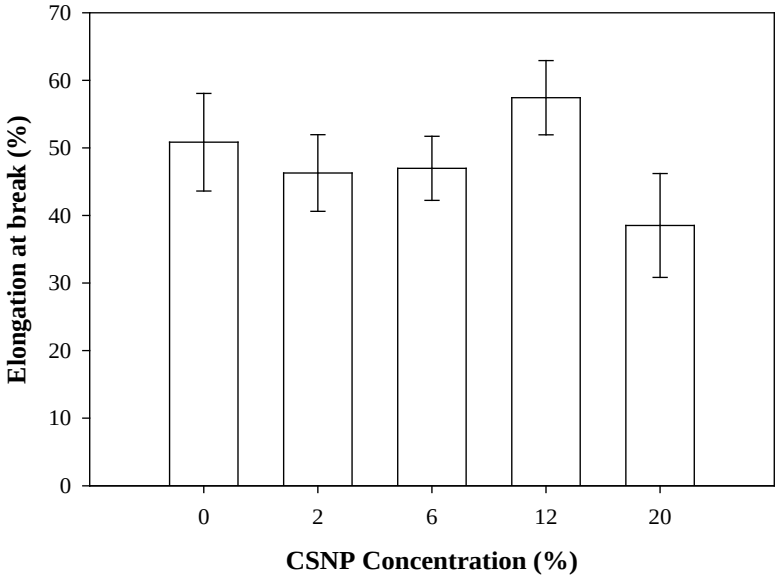

Figure 4.18. Elongation results of WPI films incorporated at different ratios

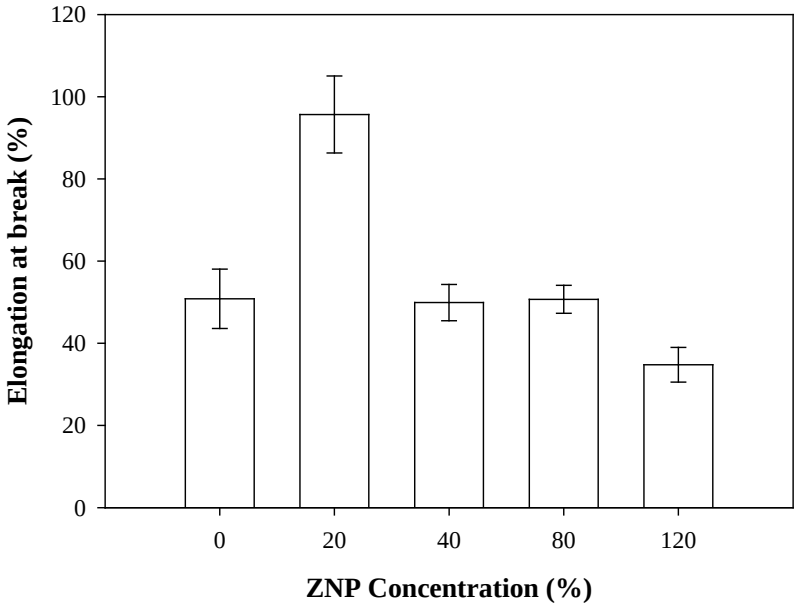

Figure 4.19. Elongation values of ZNP loaded WPI films at different concentrations

Incorporation of nanoparticles also increased the elastic modulus (EM) of the films as can be seen in Figure 4.20 and Figure 4.21. The highest CSNP loading level (20%) increased the EM by 312% and reached to 269.78 MPa whereas 120% ZNP loading increased the EM by 478%. At 20% loading, the EM of CSNP loaded WPI film was 257% higher than that of ZNP loaded film. Again, this could be attributed to closer interaction between negatively charged WPI and positively charged CSNP where nanoparticles acted as reinforcing sites in the matrix and contributed to load distribution under stress.

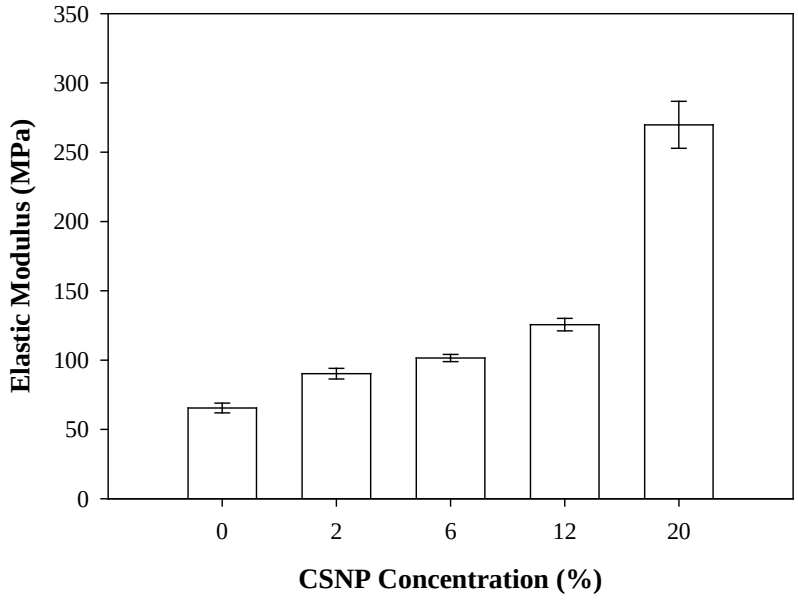

Figure 4.20. Elastic modulus results of WPI films incorporated at different ratios

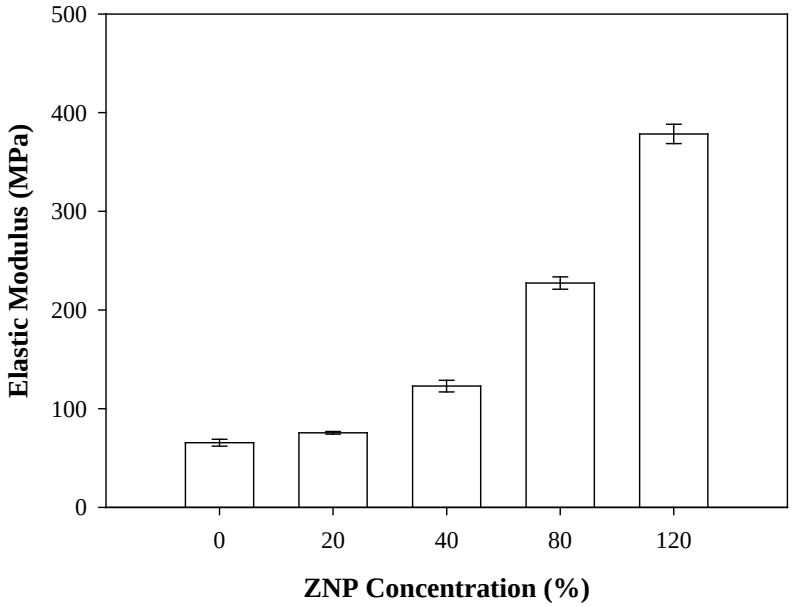

Figure 4.21. Elastic modulus of ZNP loaded WPI films at different concentrations

The results indicated that although CSNP/WPI films at 20 % loading showed better results in terms of mechanical properties than the ZNP/WPI films, more enhancement in the mechanical properties of the WPI films were obtained with the addition of ZNP. This is mainly due to better distribution of ZNP compared to CSNP which allowed much higher loading without losing the enhancement in the mechanical properties.

In literature, the mechanical properties of WPI films were tried to be improved with the inorganic nanoparticles like titania (TiO_2), clay and ZnO. Kadam et al. (2013) added silica coated titania nanoparticles and found an increase in tensile strength from 1.03 to 1.18 MPa (15% increase); in elastic modulus from 19 to 35 MPa (84% increase). Li et al. (2011) also used titania as a reinforcing agent and maximum tensile strength reached was 10.2 MPa (67% increment) and with 10% increase in elongation with the addition of 0.25% TiO_2. However, no improvement on water vapor barrier properties was seen with this composition. Zhou et al. (2009) added 0.5% TiO_2 and reached maximum strength of 2.38 MPa (41% increment) and elongation 54.08% (no change). On the other hand, addition of clay in WPI exhibited adverse effect in terms of mechanical strength in the study of Sothornvit et al. (2010). As clay content increased, tensile strength decreased by 43 % from 3.5 MPa to 2 MPa and consequently elongation increased to 60% (20% increment). Sothornvit et al. (2009) also investigated different clay types. No significant changes for mechanical strength (3.40 MPa) and elongation

(50.9%) were observed for Cloisite Na^+ and Cloisite 30B. As for Cloisite 20A, tensile strength and elongation decreased. The comparison of the results obtained in this study with the literature findings are shown in Figure 4.22. It was seen that improvements in the mechanical strength of the WPI films with the CSNP and ZNP loading is higher compared to other WPI nanocomposite films investigated in the literature.

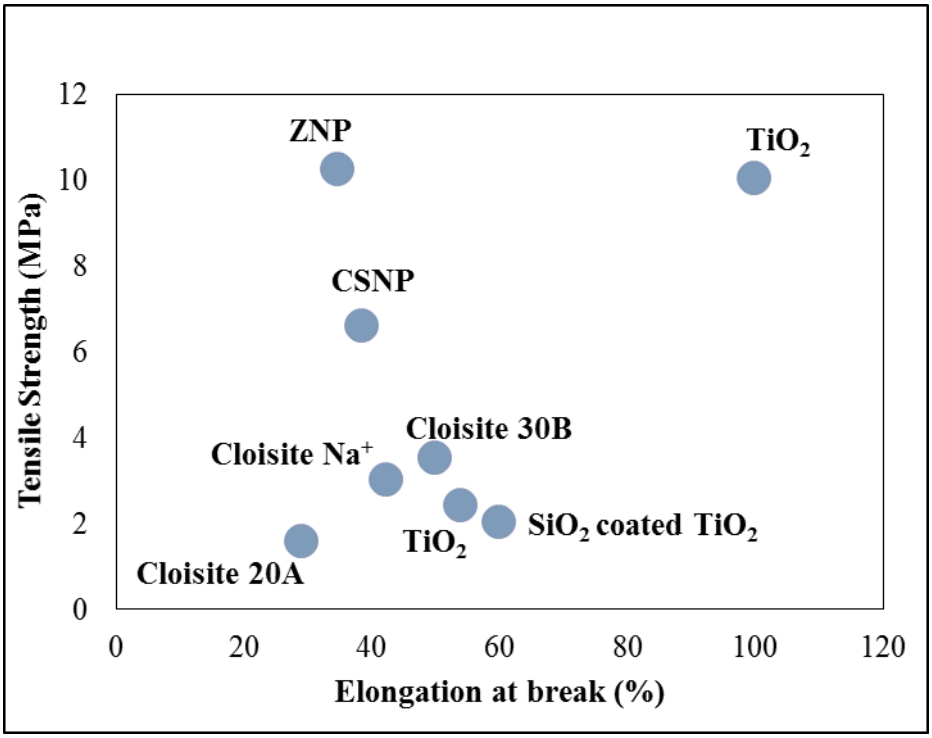

Figure 4.22. Comparison of the mechanical properties of WPI films incorporated with different nanoparticles

4.2.3. Water Vapor Permeability

Water vapor permeability (WVP) is one of the most important factors for packaging films in regard to prevention of moisture transfer between surrounding atmosphere and food. Thus, the packaging material is expected to have a low WVP for most of the packaging applications.

In literature, permeation tests were usually performed with a large relative humidity step, hence, water vapor permeabilities reported do not represent true barrier properties of the films. When the relatively humidity is increased from 0 to a high value, due to strong hydrophilic nature of the WPI, the film swells significantly which causes

diffusion coefficient to vary with concentration. Consequently, constant diffusivity and constant film thickness assumptions used in deriving Equation 2.5 are no longer valid and the WVP calculated from Equation 2.5 becomes erroneous. Being aware of this fact, in this study relative humidity was set to 25% during permeability measurement and thicknesses of the films were measured after permeation test to ensure that swelling of the film was negligible.

Figure 4.23 illustrates that the WVP of WPI films decreased gradually as CSNP concentration increased. The lowest WVP was observed at 20% CSNP loading which decreased the WVP of pure WPI film by 57%.

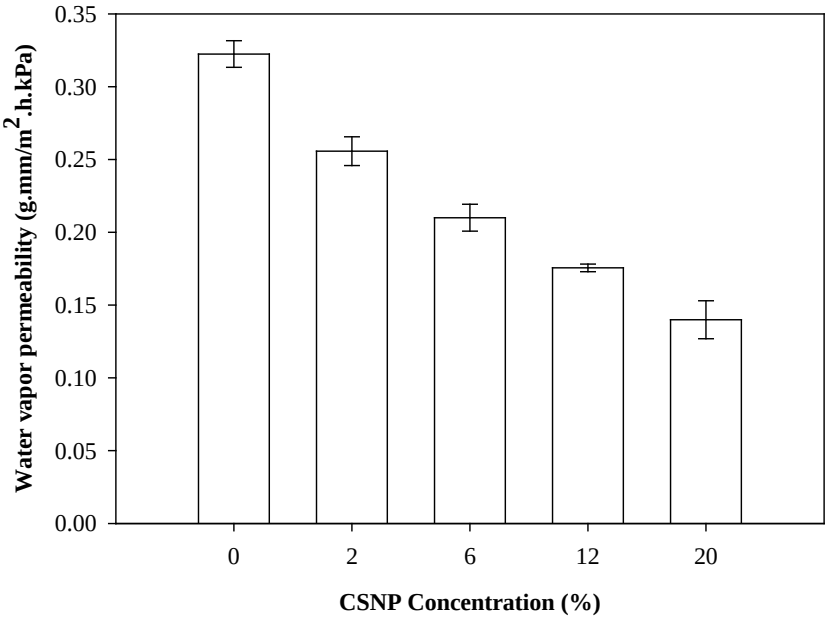

Figure 4.23. WVP of CSNP loaded WPI films

For ZNP loaded WPI films, the results are presented in Figure 4.24. Rapid decrease in WVP was observed with the increased ZNP concentration. The lowest WVP was obtained by adding 120% ZNP causing 84% decrease in WVP of the pure WPI film. As in the case of mechanical properties, higher loading concentration of ZNP allowed to achieve better barrier properties for pure WPI film compared to CSNP addition. Results showed that ZNP is more effective than CSNP in decreasing permeability of water through WPI films due to more hydrophobic nature of zein and better dispersion of the ZNPs in the protein matrix compared to CSNPs.

In literature, Li et al. (2011) reported 9.4% decrease in WVP of the WPI film with 1% TiO_2 addition. Although Zhou et al. (2009) reported 70% decrease in WVP of

the WPI film with 4% TiO_2 addition, the mechanical properties at this loading level decreased. Sothornvit et al. (2009) did not observe any gain in the barrier property of the WPI film by adding three different types of clay at a level of 5%. In another work, 20g Cloisite 30B clay addition decreased the WVP of WPI by 40%; Cloisite Na^+ by 29%; Cloisite 30B by 16%. Cloisite 20A did not change the WVP of WPI film significantly (Sothornvit et al. 2010). The comparison with the other studies indicates that CSNP and ZNP addition to WPI dramatically decreased the WVP of the films as well as increased the tensile strength and elastic modulus without changing flexibility of the film. Thus, the WPI nanocomposites prepared in this study with the nanoparticles synthesized show better mechanical and barrier properties when compared with other studies.

Permeability through a polymer film depends on two diffusivity and solubility which represent the kinetic and thermodynamic factor, respectively. Several parameters like thickness of the material, polarity and homogeneity of the film, type of the plasticizer, crystallinity and fractional free volume, hydrophobic/hydrophilic nature and temperature affects the permeation rate of the film (Massey 2003). In order to determine factors which are effective in determining barrier properties of the films, further investigations were conducted to observe the changes in hydrophilic nature, fractional free volume and crystallinity of the WPI films upon nanoparticle addition. The results are discussed in the following sections.

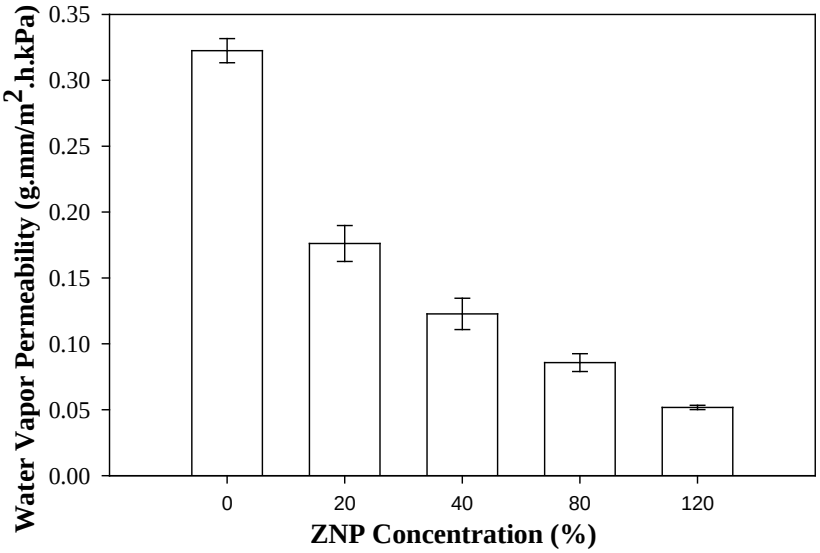

Figure 4.24. WVP of WPI films loaded with ZNP at different concentrations

4.2.4. Contact Angle Measurement

Surface wetting properties is a good indicator of the tendency of films to absorb moisture or water. Hydrophobicity of the surface is usually measured with contact angle of a water droplet on film surface. In general, initial contact angles of droplet are reported and films with higher contact angle exhibit higher hydrophobicity leading to decrease in the sensitivity of the film to moisture. Hydrophilicity of WPI leads to swelling of the film as stated before and causes incorrect contact angle measurements since swelling can contribute to change in shape and volume of drop. Kokoszka et al. (2010b) studied the effect of polymer and plasticizer amount on the wetting properties of WPI films by contact angle measurements and reported initial contact angles, absorption time and rate. Drop volume of the films first decreased with time but increased after 30 s due to film swelling. To better evaluate the hydrophilic character of the films, the rate of absorption of water ($\dot{m}_{abs}$) into the film was calculated from the change in drop volume with time using Equation 4.1. Evaporation of water during measurement was taken into account by considering the change in volume of water dropped onto impermeable aluminum foil.

$$\dot{m}_{Abs} = \rho\left[\frac{dV_{droplet}}{dt} - \frac{dV_{ev}}{dt}\right] \tag{4.1}$$

In this equation, dV_{ev} is variation of droplet volume during time dt on aluminum foil and $dV_{Droplet}$ is droplet volume change during the same time period on the WPI films. Figure 4.25 shows that the rate of absorption of water into the WPI film is significantly higher than that into the nanoparticle loaded WPI films. This result clearly indicates the reduction in the hydrophilic character of the films through nanoparticle addition allows to improve the barrier properties of the WPI films.

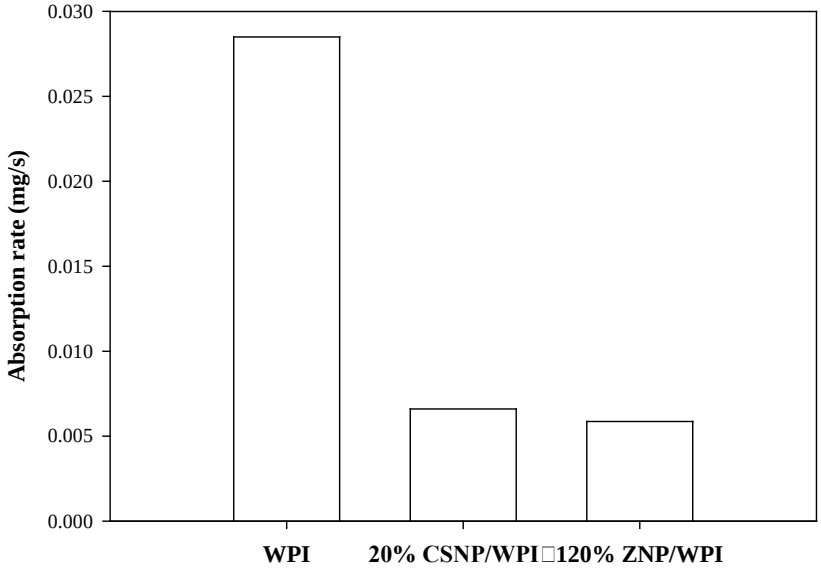

Figure 4.25. Water absorption rates of pure WPI, CSNP and ZNP loaded WPI films

4.2.5. Viscoelastic Properties

Changes in viscoelastic properties of the WPI films with nanoparticle loadings were observed with dynamic mechanical analysis (DMA). Storage and loss modulus data can be used to get some information about possible interaction/bonding between the nanoparticle and protein matrix (Menard 2008). Comparison of storage and loss moduli of the pure WPI, 120% ZNP and 20% CSNP loaded WPI films shown in Figure 4.26 and Figure 4.27, respectively showed increase in storage and loss modulus of pure WPI films with both nanoparticle additions. It was also observed that transition regions of CSNP and ZNP loaded WPI films broadened compared to that of the pure WPI film. According to Ferry (1980), in cases where particles are bridged to each other by polymer chains and act as multiple cross-links as well as rigid occupier of space, storage and especially loss modulus are increased in the rubbery zone and transition zone is broadened. Based on this argument, it was concluded that both nanoparticle addition decreased the free volume in the WPI film, however, the decrease was found much higher with CSNP addition which can be attributed to strong interaction between CSNP and WPI as previously shown with AFM, SEM and STEM images in Figure 4.10, Figure 4.12 and Figure 4.13.

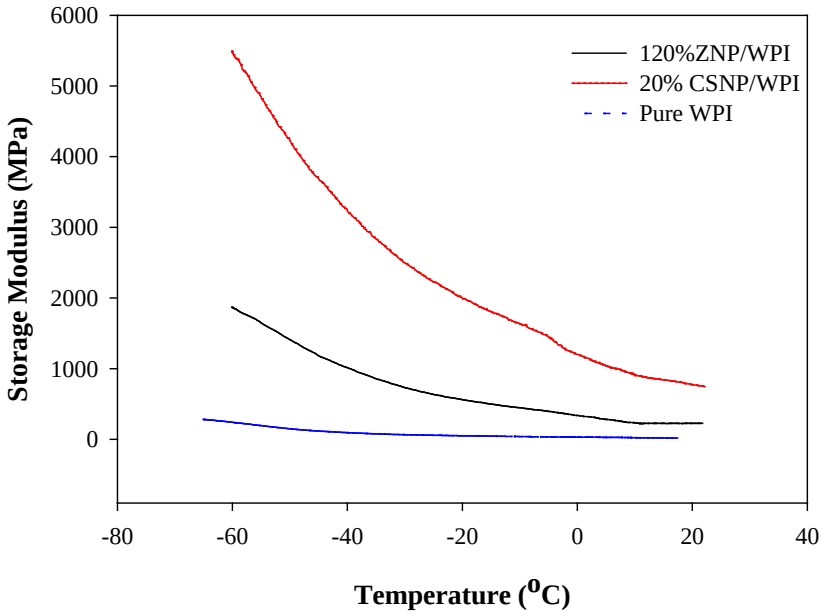

Figure 4.26. Storage modulus of pure WPI and nanoparticle loaded WPI films

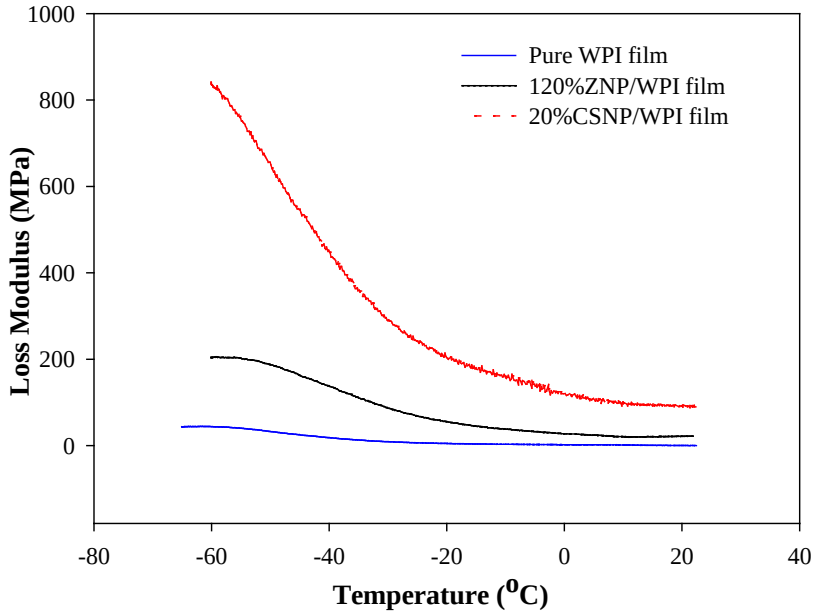

Figure 4.27. Loss modulus of pure WPI and nanoparticle loaded WPI films

Another parameter that can be calculated from DMA measurements is dynamic viscosity which is defined as loss modulus divided by angular frequency (Equation 4.2)

$$\eta' = G'' / w \quad (4.2)$$

and the results are shown in Figure 4.28. Viscosity can be directly correlated to free volume by Doolittle equation (Equation 4.3):

$$\ln \boldsymbol{\eta} = \ln A + B\,(v-v_f) / v \quad (4.3)$$

where $\boldsymbol{\eta}$ is the viscosity, v and v_f are total volume and free volume of the system, respectively, and A and B are constants (Gabbott 2008).

As it can be seen from the Doolittle equation, viscosity increases as fractional free volume decreases. In Figure 4.28, it was clearly observed that dynamic viscosity increased by addition of nanoparticles to pure WPI film. It is also observed that although amount of ZNP loading was much higher than CSNP loading, viscosity of 20% CSNP/WPI film was much higher than 120% ZNP/WPI film. This result explains why WVP values of 20% CSNP or 20% ZNP loaded WPI films are similar. Although ZNP has more hydrophobic character than CSNP, much lower fractional free volume in CSNP loaded films compensates the disadvantage of CSNP due to its hydrophilic nature.

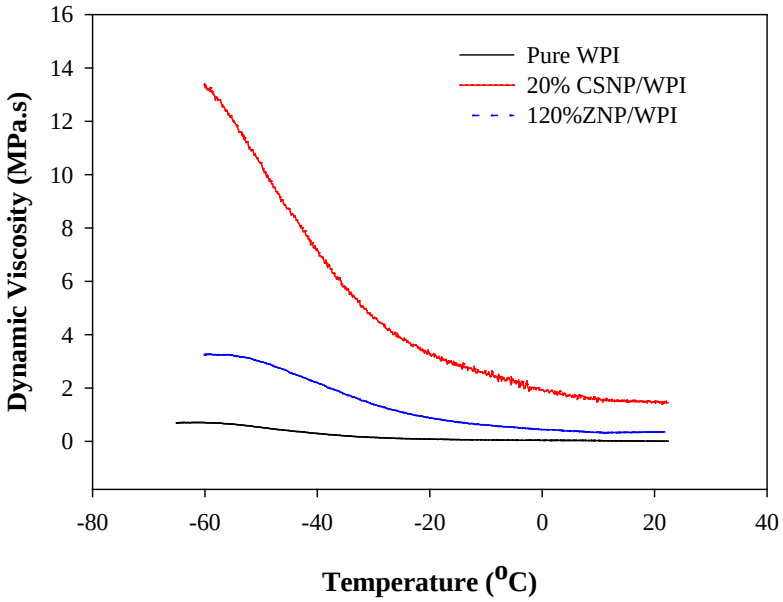

Figure 4.28. Comparison of the dynamic viscosities of the pure WPI and nanoparticle loaded WPI films

4.2.6. Differential Scanning Calorimetry (DSC)

Crystallinity of the structure affects the permeability of the film since water vapor only diffuses through amorphous regions. Increased crystalline regions in the structure would lead to decrease in permeability by preventing water vapor passed through. DSC was performed in order to see the changes in crystallinity of the WPI films with the addition of nanoparticles. When the heat flow versus temperature graph was plotted (Figure 4.29) it was observed that all films showed endothermic peak with different peak areas.

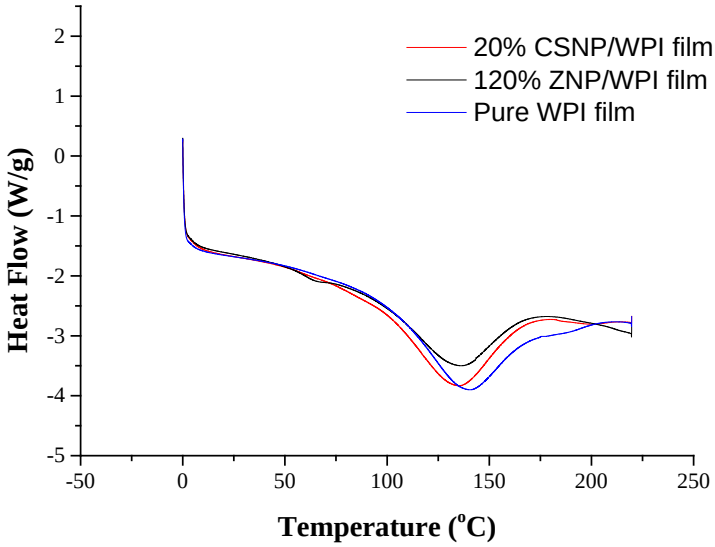

Figure 4.29. Changes on the heat flow of the films with increased temperature

When the peak area was integrated, heat of fusion was found for each film which are listed in Table 4.4. Heat of fusion which corresponds to the amount of heat necessary to melt the crystals in the films was correlated with the crystallinity of the films. Heat of fusion in 20 % CSNP added WPI film was found higher than that of pure WPI film indicating increased crystalline content with CSNP addition since chitosan has a semicrystalline structure. As expected, addition of amorphous ZNP did not change the crystallinity of WPI film. This is another reason for obtaining similar WVP values by adding 20% CSNP or 20% ZNP into WPI film.

Table 4.4. Heat of fusion values of pure WPI and nanoparticle loaded WPI films with highest loading levels

	Heat of Fusion (J/g)
Pure WPI film	94.9
20% CSNP/WPI	122.7
120% ZNP/WPI	90.4

The results indicate that improvements in barrier properties of CSNP added WPI films were due to decreased free volume and increased crystallinity of the WPI. On the other hand, improvements of ZNP loaded WPI films were due to incorporation of hydrophobic nanoparticles and homogeneous distribution.

4.2.7. Antibacterial Properties

Antibacterial properties of the films were investigated with disc diffusion method against *E.coli* and results are shown in Figure 4.30. As expected, no clear zone formation was observed around the pure WPI and ZNP loaded WPI films since there is no antimicrobial agent released from the films. On the other hand, the area which was in contact with the CSNP/WPI nanocomposite film was clear as shown in Figure 4.30 indicating that CSNP stopped the growth of bacteria and killed bacteria in contact with film surface. In contrast, bacteria formation was observed in the region which was in contact with pure WPI and ZNP loaded WPI films. It revealed that WPI and zein had no effect on inhibition of *E.Coli.*

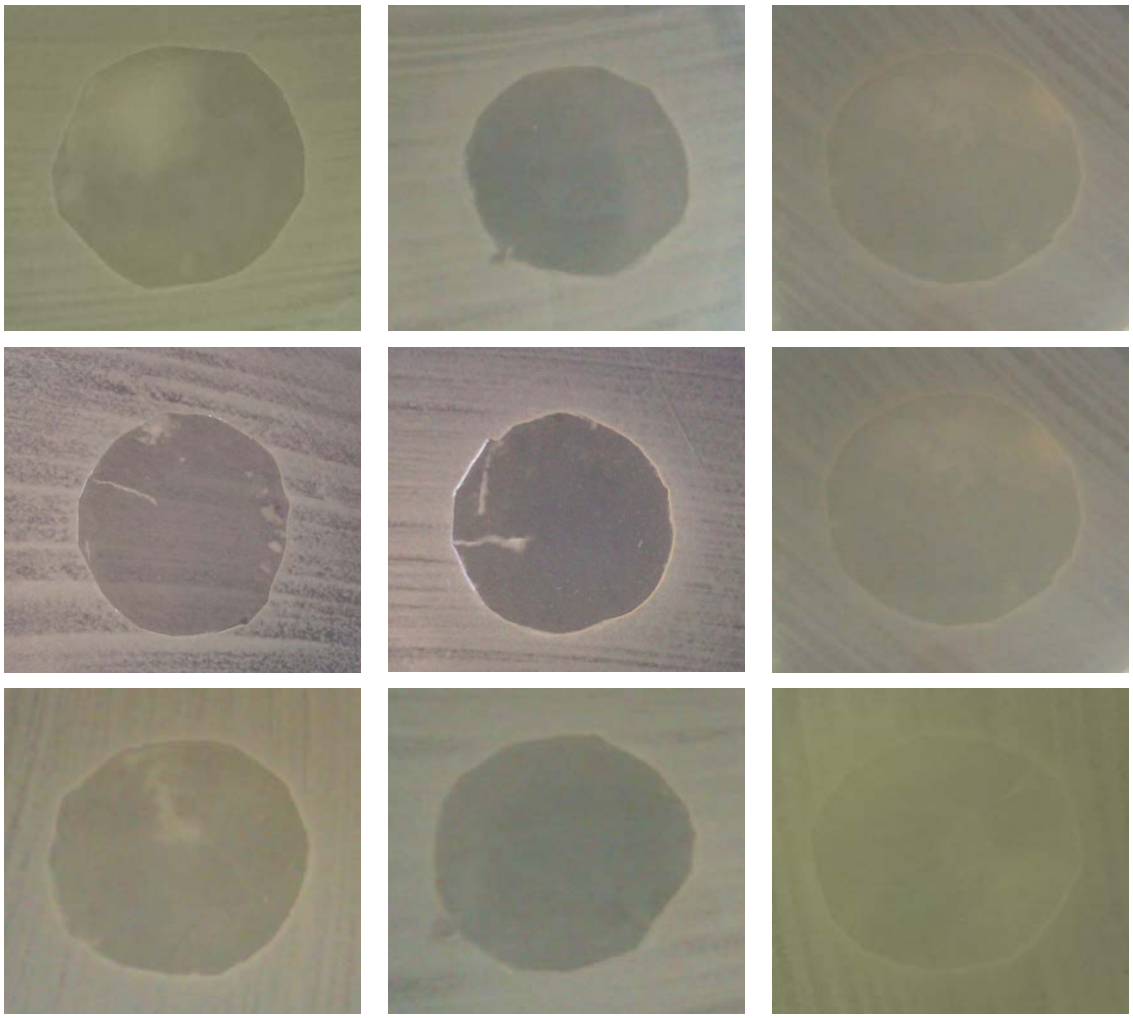

Pure WPI film CSNP/WPI film ZNP/WPI film

Figure 4.30. Images of the disc diffusion test for pure WPI (control), CSNP/WPI films and ZNP/WPI films

Illustration of antibacterial activity of chitosan can be seen in Figure 4.31. Antibacterial efficiency of CS was explained in literature due to the cationic structure of CS which causes electrostatic interaction between positively charged amino groups of CS and negatively charged compounds in cell membrane. This causes the loss of integrity and changes the permeability of the cell and spoil the microbial cell as a consequence of released intracellular substances (Rabea et al. 2003; Cota-Arriola et al. 2013).

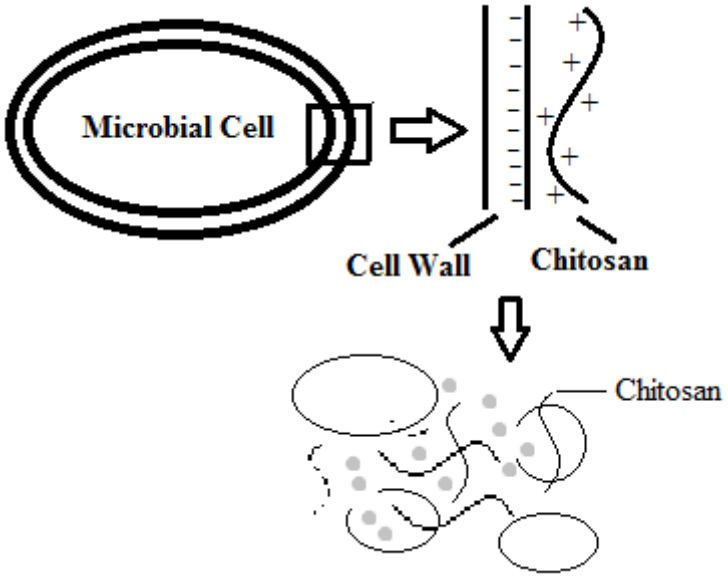

Figure 4.31. Illustration of the antibacterial activity mechanism of CS

CHAPTER 5

CONCLUSION

In this study, glycerol plasticized WPI nanocomposites were produced by incorporation of chitosan and zein nanoparticles. Best performances were recorded for 20% CSNP and 120% ZNP loaded WPI films. As a result of both nanoparticle addition, water vapor permeability of the WPI films decreased significantly while tensile strength and elastic modulus increased without any change in elongation values. Improvements in the barrier properties of the WPI films with chitosan nanoparticle addition are mainly due to decrease in fractional free volume and increase in the crystallinity of the film. On the other hand, the dominant factor for the decrease in the WVP of the WPI films upon ZNP addition is the hydrophobic nature of zein. ZNPs was found more effective than CSNPs in improving both barrier and mechanical properties of the WPI films as a consequence of much higher loading levels achieved with ZNPs. The unique advantage of CSNP/WPI composite films is their antibacterial activity which was not observed in pure WPI and zein nanoparticle loaded WPI films.

In conclusion, poor mechanical and moisture barrier properties of the WPI films were improved via addition of nanoparticles. Especially zein nanoparticles loaded WPI films could be a good candidate as biopolymer based packaging material with improved water vapor barrier and mechanical properties.

REFERENCES

Agnihotri, S. A., N. N. Mallikarjuna, and T. M. Aminabhavi. 2004. "Recent advances on chitosan-based micro- and nanoparticles in drug delivery." *Journal of Controlled Release* 100 (1):5-28.

Anker, M., M. Stading, and A. M. Hermansson. 1999. "Effects of pH and the gel state on the mechanical properties, moisture contents, and glass transition temperatures of whey protein films." *Journal of Agricultural and Food Chemistry* 47 (5):1878-1886.

Brindle, L. P., and J. M. Krochta. 2008. "Physical Properties of Whey Protein-Hydroxypropylmethylcellulose Blend Edible Films." *Journal of Food Science* 73 (9):E446-E454.

Calvo, P., C. RemunanLopez, J. L. VilaJato, and M. J. Alonso. 1997. "Novel hydrophilic chitosan-polyethylene oxide nanoparticles as protein carriers." *Journal of Applied Polymer Science* 63 (1):125-132.

Chaplin, L. C., and R. L. J. Lyster. 1986. "Irreversible Heat Denaturation of Bovine Alpha-Lactalbumin." *Journal of Dairy Research* 53 (2):249-258.

Ciesla, K., S. Salmieri, and M. Lacroix. 2006a. "gamma-irradiation influence on the structure and properties of calcium caseinate-whey protein isolate based films. Part 1. Radiation effect on the structure of proteins gels and films." *Journal of Agricultural and Food Chemistry* 54 (17):6374-6384.

Ciesla, K., S. Salmieri, and M. Lacroix. 2006b. "gamma-irradiation influence on the structure and properties of calcium caseinate-whey protein isolate based films. Part 2. Influence of polysaccharide addition and radiation treatment on the structure and functional properties of the films." *Journal of Agricultural and Food Chemistry* 54 (23):8899-8908.

Cota-Arriola, O., M. O. Cortez-Rocha, A. Burgos-Hernandez, J. M. Ezquerra-Brauer, and M. Plascencia-Jatomea. 2013. "Controlled release matrices and micro/nanoparticles of chitosan with antimicrobial potential: development of new strategies for microbial control in agriculture." *Journal of the Science of Food and Agriculture* 93 (7):1525-1536.

de Moura, M. R., F. A. Aouada, R. J. Avena-Bustillos, T. H. McHugh, J. M. Krochta, and L. H. C. Mattoso. 2009. "Improved barrier and mechanical properties of novel hydroxypropyl methylcellulose edible films with chitosan/tripolyphosphate nanoparticles." *Journal of Food Engineering* 92 (4):448-453.

Dudhani, A. R., and S. L. Kosaraju. 2010. "Bioadhesive chitosan nanoparticles: Preparation and characterization." *Carbohydrate Polymers* 81 (2):243-251.

Erdohan, Z. O., and K. N. Turhan. 2005. "Barrier and mechanical properties of methyicellulose-whey protein films." *Packaging Technology and Science* 18 (6):295-302.

Fairley, P., F. J. Monahan, J. B. German, and J. M. Krochta. 1996. "Mechanical properties and water vapor permeability of edible films from whey protein isolate and sodium dodecyl sulfate." *Journal of Agricultural and Food Chemistry* 44 (2):438-443.

Fan, W., W. Yan, Z. S. Xu, and H. Ni. 2012. "Formation mechanism of monodisperse, low molecular weight chitosan nanoparticles by ionic gelation technique." *Colloids and Surfaces B-Biointerfaces* 90:21-27.

Fang, Y., M. A. Tung, I. J. Britt, S. Yada, and D. G. Dalgleish. 2002. "Tensile and barrier properties of edible films made from whey proteins." *Journal of Food Science* 67 (1):188-193.

Ferry, J.D. 1980. *Viscoelastic Properties of Polymers*: John Wiley&Sons.

Gabbott, P. 2008. *Principles and Applications of Thermal Analysis*: Blackwell Publishing Ltd.

Gounga, M. E., S. Y. Xu, and Z. Wang. 2007. "Whey protein isolate-based edible films as affected by protein concentration, glycerol ratio and pullulan addition in film formation." *Journal of Food Engineering* 83 (4):521-530.

Grenha, A. 2012. "Chitosan nanoparticles: a survey of preparation methods." *Journal of Drug Targeting* 20 (4):291-300.

Harper, B. A., S. Barbut, L. T. Lim, and M. F. Marcone. 2013. "Characterization of 'wet' alginate and composite films containing gelatin, whey or soy protein." *Food Research International* 52 (1):452-459.

Hong, S. I., and J. M. Krochta. 2003. "Oxygen barrier properties of whey protein isolate coatings on polypropylene films." *Journal of Food Science* 68 (1):224-228.

Hong, S. I., and J. M. Krochta. 2004. "Whey protein isolate coating on LDPE film as a novel oxygen barrier in the composite structure." *Packaging Technology and Science* 17 (1):13-21.

Hong, S. I., and J. M. Krochta. 2006. "Oxygen barrier performance of whey-protein-coated plastic films as affected by temperature, relative humidity, base film and protein type." *Journal of Food Engineering* 77 (3):739-745.

Hong, Y. H., and L. K. Creamer. 2002. "Changed protein structures of bovine beta-lactoglobulin B and alpha-lactalbumin as a consequence of heat treatment." *International Dairy Journal* 12 (4):345-359.

Hu, B., C. L. Pan, Y. Sun, Z. Y. Hou, H. Ye, B. Hu, and X. X. Zeng. 2008. "Optimization of fabrication parameters to produce chitosan-tripolyphosphate nanoparticles for delivery of tea catechins." *Journal of Agricultural and Food Chemistry* 56 (16):7451-7458.

Ikeda, S., and V. J. Morris. 2002. "Fine-stranded and particulate aggregates of heat-denatured whey proteins visualized by atomic force microscopy." *Biomacromolecules* 3 (2):382-389.

Janes, K. A., P. Calvo, and M. J. Alonso. 2001. "Polysaccharide colloidal particles as delivery systems for macromolecules." *Advanced Drug Delivery Reviews* 47 (1):83-97.

Janjarasskul, T., D. J. Rauch, K. L. McCarthy, and J. M. Krochta. 2014. "Barrier and tensile properties of whey protein-candelilla wax film/sheet." *Lwt-Food Science and Technology* 56 (2):377-382.

Jelen, P. 2003. "Whey Processing: Utilization and products." In *Encyclopedia of Dairy Sciences*, edited by H. Roginski, J.W. Fuquay and P.F. Fox, 2739-2745. New York: Academic Press.

Jiang, Y. F., Y. X. Li, Z. Chai, and X. J. Leng. 2010. "Study of the Physical Properties of Whey Protein Isolate and Gelatin Composite Films." *Journal of Agricultural and Food Chemistry* 58 (8):5100-5108.

Kadam, D. M., M. Thunga, S. Wang, M. R. Kessler, D. Grewell, B. Lamsal, and C. X. Yu. 2013. "Preparation and characterization of whey protein isolate films reinforced with porous silica coated titania nanoparticles." *Journal of Food Engineering* 117 (1):133-140.

Kasaai, M. R. 2011. "The Use of Various Types of NMR and IR Spectroscopy for Structural Characterization of Chitin and Chitosan." In *Chitin, Chitosan, Oligosaccharides and Their Derivatives: Biological Activities and Applications*, edited by Se-Kwon Kim. Boca Raton: CRC Press.

Khwaldia, K., C. Perez, S. Banon, S. Desobry, and J. Hardy. 2004. "Milk proteins for edible films and coatings." *Critical Reviews in Food Science and Nutrition* 44 (4):239-251.

Kilara, A., and M.N. Vaghela. 2004. "Whey proteins." In *Proteins in Food Processing*, edited by R.Y. Yada, 72-99. Cambridge: Woodhead Publishing.

Kim, Se-Kwon. 2011. *Chitin, chitosan, oligosaccharides and their derivatives : biological activities and applications*. Boca Raton: Taylor & Francis.

Kokoszka, S., F. Debeaufort, A. Lenart, and A. Voilley. 2010a. "Liquid and vapour water transfer through whey protein/lipid emulsion films." *Journal of the Science of Food and Agriculture* 90 (10):1673-1680.

Kokoszka, S., F. Debeaufort, A. Lenart, and A. Voilley. 2010b. "Water vapour permeability, thermal and wetting properties of whey protein isolate based edible films." *International Dairy Journal* 20 (1):53-60.

Lee, J. W., S. M. Son, and S. I. Hong. 2008. "Characterization of protein-coated polypropylene films as a novel composite structure for active food packaging application." *Journal of Food Engineering* 86 (4):484-493.

Li, K. K., S. W. Yin, Y. C. Yin, C. H. Tang, X. Q. Yang, and S. H. Wen. 2013. "Preparation of water-soluble antimicrobial zein nanoparticles by a modified antisolvent approach and their characterization." *Journal of Food Engineering* 119 (2):343-352.

Li, Y. X., Y. F. Jiang, F. Liu, F. Z. Ren, G. H. Zhao, and X. J. Leng. 2011. "Fabrication and characterization of TiO2/whey protein isolate nanocomposite film." *Food Hydrocolloids* 25 (5):1098-1104.

Mahalik, N. P., and A. N. Nambiar. 2010. "Trends in food packaging and manufacturing systems and technology." *Trends in Food Science & Technology* 21 (3):117-128.

Massey, L.K. 2003. *Permeability Properties of Plastics and Elastomers: A Guide to Packaging and Barrier Materials*. Second Edition ed. USA: Plastics Design Library.

Mchugh, T. H., J. F. Aujard, and J. M. Krochta. 1994. "Plasticized Whey-Protein Edible Films - Water-Vapor Permeability Properties." *Journal of Food Science* 59 (2):416-+.

Mchugh, T. H., and J. M. Krochta. 1994a. "Sorbitol-Plasticized Vs Glycerol-Plasticized Whey-Protein Edible Films - Integrated Oxygen Permeability and Tensile Property Evaluation." *Journal of Agricultural and Food Chemistry* 42 (4):841-845.

Mchugh, T. H., and J. M. Krochta. 1994b. "Water-Vapor Permeability Properties of Edible Whey Protein-Lipid Emulsion Films." *Journal of the American Oil Chemists Society* 71 (3):307-312.

Mehra, R., and B.T. O'Kennedy. 2008. "Separation of Beta-Lactoglobulin from Whey: Its physico-chemical properties and potential uses." In *Whey Processing, Functionality and Health Benefits*, edited by C.I. Onwulata and P.J. Huth, 39-62. IFT Press-Blackwell Publishing.

Menard, H.P. 2008. *Dynamic Mechanical Analysis: A Practical Introduction*: CRC Press.

Mi, F. L., S. S. Shyu, C. Y. Kuan, S. T. Lee, K. T. Lu, and S. F. Jang. 1999. "Chitosan-polyelectrolyte complexation for the preparation of gel beads and controlled release of anticancer drug. I. Effect of phosphorous polyelectrolyte complex and enzymatic hydrolysis of polymer." *Journal of Applied Polymer Science* 74 (7):1868-1879.

Min, S. C., T. Janjarasskul, and J. M. Krochta. 2009. "Tensile and moisture barrier properties of whey protein-beeswax layered composite films." *Journal of the Science of Food and Agriculture* 89 (2):251-257.

Mittal, V. 2009. "Barrier Properties of Composite Materials." In *Barrier Properties of Polymer Clay Nanocomposites*, edited by V. Mittal. Nova Science Publishers.

Moditsi, M., A. Lazaridou, T. Moschakis, and C. G. Biliaderis. 2014. "Modifying the physical properties of dairy protein films for controlled release of antifungal agents." *Food Hydrocolloids* 39:195-203.

Onwulata, C.I., and P.J. Huth. 2008. *Whey Processing, Functionality and Health Benefits*: IFT Press-Blackwell Publishing.

Patel, A. R., E. C. M. Bouwens, and K. P. Velikov. 2010. "Sodium Caseinate Stabilized Zein Colloidal Particles." *Journal of Agricultural and Food Chemistry* 58 (23):12497-12503.

Paulsson, M., and P. Dejmek. 1990. "Thermal-Denaturation of Whey Proteins in Mixtures with Caseins Studied by Differential Scanning Calorimetry." *Journal of Dairy Science* 73 (3):590-600.

Perez-Gago, M. B., and J. M. Krochta. 2001. "Lipid particle size effect on water vapor permeability and mechanical properties of whey protein/beeswax emulsion films." *Journal of Agricultural and Food Chemistry* 49 (2):996-1002.

Perez-Gago, M. B., M. Serra, M. Alonso, M. Mateos, and M. A. del Rio. 2005. "Effect of whey protein- and hydroxypropyl methylcellulose-based edible composite coatings on color change of fresh-cut apples." *Postharvest Biology and Technology* 36 (1):77-85.

Petersen, K., P. V. Nielsen, G. Bertelsen, M. Lawther, M. B. Olsen, N. H. Nilsson, and G. Mortensen. 1999. "Potential of biobased materials for food packaging." *Trends in Food Science & Technology* 10 (2):52-68.

Prommakool, A., T. Sajjaanantakul, T. Janjarasskul, and J. M. Krochta. 2011. "Whey protein-okra polysaccharide fraction blend edible films: tensile properties, water vapor permeability and oxygen permeability." *Journal of the Science of Food and Agriculture* 91 (2):362-369.

Rabea, E. I., M. E. T. Badawy, C. V. Stevens, G. Smagghe, and W. Steurbaut. 2003. "Chitosan as antimicrobial agent: Applications and mode of action." *Biomacromolecules* 4 (6):1457-1465.

Ramos, O. L., I. Reinas, S. I. Silva, J. C. Fernandes, M. A. Cerqueira, R. N. Pereira, A. A. Vicente, M. F. Pocas, M. E. Pintado, and F. X. Malcata. 2013. "Effect of whey protein purity and glycerol content upon physical properties of edible films manufactured therefrom." *Food Hydrocolloids* 30 (1):110-122.

Rhim, J. W., and P. K. W. Ng. 2007. "Natural biopolymer-based nanocomposite films for packaging applications." *Critical Reviews in Food Science and Nutrition* 47 (4):411-433.

Sabato, S. F., B. Ouattara, H. Yu, G. D'Aprano, C. Le Tien, M. A. Mateescu, and M. Lacroix. 2001. "Mechanical and barrier properties of cross-linked soy and whey protein based films." *Journal of Agricultural and Food Chemistry* 49 (3):1397-1403.

Sharma, S., and I. Luzinov. 2013. "Whey based binary bioplastics." *Journal of Food Engineering* 119 (3):404-410.

Shukla, R., and M. Cheryan. 2001. "Zein: the industrial protein from corn." *Industrial Crops and Products* 13 (3):171-192.

Sothornvit, R., S. I. Hong, D. J. An, and J. W. Rhim. 2010. "Effect of clay content on the physical and antimicrobial properties of whey protein isolate/organo-clay composite films." *Lwt-Food Science and Technology* 43 (2):279-284.

Sothornvit, R., and J. M. Krochta. 2000. "Oxygen permeability and mechanical properties of films from hydrolyzed whey protein." *Journal of Agricultural and Food Chemistry* 48 (9):3913-3916.

Sothornvit, R., J. W. Rhim, and S. I. Hong. 2009. "Effect of nano-clay type on the physical and antimicrobial properties of whey protein isolate/clay composite films." *Journal of Food Engineering* 91 (3):468-473.

Tharanathan, R. N. 2003. "Biodegradable films and composite coatings: past, present and future." *Trends in Food Science & Technology* 14 (3):71-78.

Tunick, M.H. 2008. "Whey protein production and utilization: A Brief History." In *Whey Processing, Functionality and Health Benefits*, edited by C.I. Onwulata and P.J. Huth, 1-13. IFT Press-Blackwell Publishing.

Wang, J., J. J. Shang, F. Z. Ren, and X. J. Leng. 2010a. "Study of the physical properties of whey protein: sericin protein-blended edible films." *European Food Research and Technology* 231 (1):109-116.

Wang, L. Z., M. A. E. Auty, and J. P. Kerry. 2010b. "Physical assessment of composite biodegradable films manufactured using whey protein isolate, gelatin and sodium alginate." *Journal of Food Engineering* 96 (2):199-207.

Wihodo, M., and C. I. Moraru. 2013. "Physical and chemical methods used to enhance the structure and mechanical properties of protein films: A review." *Journal of Food Engineering* 114 (3):292-302.

Woishnis, W. 1995. *Permeability and other film properties of plastics and elastomers*: Plastics Design Library.

Wu, Y., W. L. Yang, C. C. Wang, J. H. Hu, and S. K. Fu. 2005. "Chitosan nanoparticles as a novel delivery system for ammonium glycyrrhizinate." *International Journal of Pharmaceutics* 295 (1-2):235-245.

Yoo, S. R., and J. M. Krochta. 2011. "Whey protein-polysaccharide blended edible film formation and barrier, tensile, thermal and transparency properties." *Journal of the Science of Food and Agriculture* 91 (14):2628-2636.

Zhang, H. K., and G. Mittal. 2010. "Biodegradable Protein-based Films from Plant Resources: A Review." *Environmental Progress & Sustainable Energy* 29 (2):203-220.

Zhang, H., M. Oh, C. Allen, and E. Kumacheva. 2004. "Monodisperse chitosan nanoparticles for mucosal drug delivery." *Biomacromolecules* 5 (6):2461-2468.

Zhou, J. J., S. Y. Wang, and S. Gunasekaran. 2009. "Preparation and Characterization of Whey Protein Film Incorporated with TiO2 Nanoparticles." *Journal of Food Science* 74 (7):N50-N56.

Zolfi, M., F. Khodaiyan, M. Mousavi, and M. Hashemi. 2014. "Development and characterization of the kefiran-whey protein isolate-TiO2 nanocomposite films." *International Journal of Biological Macromolecules* 65:340-345.